Extended Ensemble Approach for Deriving Transferable Coarse-grained Potentials

J. W. Mullinax and W. G. Noid[†]

Department of Chemistry, The Pennsylvania State University, University Park, Pennsylvania 16802

(Dated: August 13, 2009)

Abstract

The present document has been prepared for the EPAPS system to provide supplementary material for the paper "Extended Ensemble Approach for Deriving Transferable Coarse-grained Potentials" by J. W. Mullinax and W. G. Noid submitted to the Journal of Chemical Physics. The text provides a detailed description of the calculations demonstrating the extended ensemble approach. The first figure demonstrates the sensitivity of the M2N1 and M3N1 extended ensemble potentials to the topology distribution. The remaining figures compare site-site RDFs calculated from CG MD simulations using transferable interaction potentials with the RDFs calculated from all-atom MD simulations. The systems considered in these figures correspond to the various systems described in Table III of the paper. The transferable potentials were calculated for the extended ensemble defined by the first five systems in the table. The RDFs for these systems are presented in Figs. 2-24. The transferable potentials were then tested on the subsequent systems in the table, which were not included in the parameterization. The RDFs for these systems are presented in Figs. 25-46.

I. COMPUTATIONAL DETAILS

The manuscript developed a formal framework for calculating transferable CG potential functions from an atomically detailed extended canonical ensemble. This framework identified a generalized topology-dependent PMF as the appropriate potential for a structurally consistent CG extended canonical ensemble. Moreover, this framework extended the MS-CG variational principle[1–3] to determine transferable potentials that provide optimal approximations to this topology-dependent PMF. The present section describes the computational details necessary for demonstrating this extended ensemble approach for calculating transferable potentials for CG models of binary mixtures of alcohols and alkanes.

All MD simulations were performed using the GROMACS 3.3.3 software package.[4,5] Interactions in all atomistic simulations were modeled using the OPLS all-atom (OPLS-AA) force field.[6] No bonds were constrained and a 1 fs timestep was employed in propagating the dynamics. Electrostatic interactions were modeled using the particle mesh Ewald method[7] with the real space contribution truncated at 1.2nm and van der Waals interactions were truncated at 1.2nm. A Nose-Hoover thermostat was employed to generate configurations sampling the canonical ensemble.[8,9]

For each atomistic topology, initial configurations were generated on a lattice. These configurations were then equilibrated by first performing simulations at constant temperature and constant volume, followed by simulations at 1 bar constant pressure and constant temperature using the Berendsen barostat.[10] The final configurations from these simulations were then employed in simulations sampling the canonical ensemble as described above. Data from the first 1ns of these simulations were discarded and the coordinates and forces were sampled each picosecond during the following 5ns.

In each case, an atomistic extended canonical ensemble was defined by specifying a collection of atomically detailed topologies, each representing a different molecular system. Each topology was assigned equal weight (i.e., p_γ was uniform) and the OPLS-AA force field[6] determined a potential for each topology. Independent all-atom MD simulations then sampled the canonical distribution for each atomistic topology, according to the prescription above. Configurations sampled from these simulations then provided sampled configurations for the atomistic extended canonical ensemble.

A CG representation of the atomically detailed extended canonical ensemble was then

determined by defining topology and configuration maps. The topology mapping determined the CG topologies included in the CG extended ensemble, while the configuration mapping transformed configurations for the atomistic topologies into configurations for the CG topologies. The topology mapping determined a CG topology from each atomically detailed topology by specifying the number, types, and connectivity of the sites employed in representing each molecule. Each site in the mapped CG topology represented a group of atoms in the associated atomistic topology. This group of atoms then defined the group of atoms involved in each site. No atom was involved in more than one site. The topology mapping identified two sites as "bonded" if any atom involved in the first site was bonded to an atom involved in the second site. Various topology maps were considered in the following calculations, but in each case the associated configuration mapping determined the Cartesian coordinates for each site in the CG topology as the center of mass for the atoms involved in the site. The mass of each site was defined as the net mass of the atoms involved in the site.[11] The topology and configuration mappings were applied to the configurations sampled from the atomistic simulations to determine configurations for the topologies in the CG extended ensemble. Radial distribution functions (RDFs) were then calculated for each CG topology from these configurations.

For each topology Γ included in the CG extended canonical ensemble, the approximate potential energy function $\bar{U}_\Gamma$ was assumed to be of the same form as a conventional atomistic potential energy function, including inter- and intramolecular interactions. The intermolecular potential included pair potentials between each pair of sites in distinct molecules. The CG potential function did not include long-ranged electrostatic interactions, although such a term can be readily added within the present framework.[11] The intramolecular potential included bond-stretch potentials for each pair of bonded sites, bond-angle potentials for each set of three successively bonded sites, dihedral angle potentials for each set of four successively bonded sites, and also short-ranged non-bonded pair potentials between each pair of sites in the same molecule that were separated by four or more bonds. The intramolecular potential excluded non-bonded pair interactions between sites that were separated by less than four bonds, and the non-bonded pair interactions between sites separated by four or more bonds in the same molecule were treated equivalently to non-bonded pair interactions between sites in distinct molecules. Although the present methodology does not require this approximation, distinguishing between multiple tabulated inter- and intra-molecular short-

ranged interactions would have required significant modification of the GROMACS 3.3.3 software package[4,5]

In each case, the non-bonded pair potentials were represented with discrete delta basis functions on a grid with a mesh of $\delta r = 0.004$nm and these interactions were truncated at $r_{max} = 1.5$nm.[11,12] Bond-stretch and bond-angle potentials were represented with harmonic basis functions, $U_{\zeta j}(z) = \frac{1}{2}z^2\phi_{\zeta j1} - z\phi_{\zeta j2}$, and dihedral angle potentials were represented with five terms from the Ryckaert-Bellemans series: $U_{\zeta j}(\psi) = \sum_{d=1}^{5}\phi_{\zeta jd}\left(\cos(\eta)\right)^d$, where ψ is the proper dihedral angle formed by four consecutively bonded sites and $\eta = \psi - 180^0$.[13]

The topology weighting factor was assigned a value $w_\Gamma = 1/3N_\Gamma$ for each Γ and the quantities b_D and G_{DD} defined in Eqs. (21) and (22) were then approximated for all parameters $D = 1, \ldots, N_D$ in the force field using the configurations and forces sampled from the atomistic extended canonical ensemble. The atomistic force $\mathbf{f}_{\gamma I}$ in the definition of b_D was evaluated as the net force on the atoms in topology γ that are involved in CG site I.[3,11] The function $\chi^2(\phi)$ was then minimized by solving the associated normal system of equations, Eq. (23), for the force field parameters, ϕ_D, via LU decomposition after row preconditioning the matrix, $G_{DD'}$.[14–16] Prior to preconditioning, the basis functions corresponding to interactions that were not sampled during the MD simulations were eliminated from the computation. These basis functions correspond to interactions between sites that overlap in the core excluded volume region and the magnitude of these interactions were assigned by linearly extending the calculated force into the core region.[11] The calculated force field coefficients, ϕ_D, then determine topology-independent interaction potentials that provide an optimal transferable approximation to the topology-dependent many-body PMF for the extended canonical ensemble.

These transferable interaction potentials were then employed in MD simulations for various CG topologies. By construction, the calculated CG potential energy functions were compatible with the GROMACS 3.3.3 software package.[4,5,13] The CG pair potentials were determined by numerically integrating the calculated pair forces via the trapezoid rule after linearly interpolating these tabulated forces between grid points. In addition, GROMACS 3.3.3 requires the second derivative for each pair potential, which was obtained by first computing discrete finite differences of the calculated pair forces and then smoothing these differences by performing a running average over three successive grid points. The coefficients calculated for the analytic intramolecular bonded potentials determined parameters

for analytic bonded potentials employed in the simulations.

For almost every CG topology, the final configuration sampled from simulations of the corresponding atomistic topology was mapped to determine the initial configuration for the CG MD simulations. The only exceptions to this practice were the butane-butanol systems used to test the transferable CG potentials. For these systems, the initial CG configuration was determined by mapping atomistic configurations after 1ns of NPT and 1ns of NVT equilibration of the atomistic model. Each CG topology was simulated for 10ns under the same thermodynamic conditions as the corresponding atomistic topology using the Nose-Hoover thermostat to sample the appropriate canonical ensemble.[8,9] A timestep of 1 fs was employed and all bonds were flexible in the CG MD simulations. RDFs were then calculated from the CG configurations that were sampled every 1 ps from the last 3ns of the methanol-neopentane simulations and from the last 5ns of the alkane-alcohol simulations.

References

[1] S. Izvekov and G. A. Voth, J. Phys. Chem. B **109**, 2469 (2005).

[2] S. Izvekov and G. A. Voth, J. Chem. Phys. **123**, 134105 (2005).

[3] W. G. Noid, J.-W. Chu, G. S. Ayton, V. Krishna, S. Izvekov, G. A. Voth, A. Das, and H. C. Andersen, J. Chem. Phys. **128**, 244114 (2008).

[4] E. Lindahl, B. Hess, and D. van der Spoel, J. Mol. Model. **7**, 306 (2001).

[5] D. van der Spoel, E. Lindahl, B. Hess, G. Groenhof, A. E. Mark, and H. J. C. Berendsen, J. Comp. Chem. **26**, 1701 (2005).

[6] W. L. Jorgensen, D. S. Maxwell, and J. Tirado-Rives, J. Am. Chem. Soc. **118**, 11225 (1996).

[7] T. Darden, D. M. York, and L. G. Pedersen, J. Chem. Phys. **99**, 8345 (1993).

[8] S. Nose, Mol. Phys. **52**, 255 (1984).

[9] W. G. Hoover, Phys. Rev. A **31**, 1695 (1985).

[10] H. J. C. Berendsen, J. P. M. Postma, W. F. van Gunsteren, A. DiNola, and J. R. Haak, J. Chem. Phys. **81**, 3684 (1984).

[11] W. G. Noid, P. Liu, Y. T. Wang, J.-W. Chu, G. S. Ayton, S. Izvekov, H. C. Andersen, and G. A. Voth, J. Chem. Phys. **128**, 244115 (2008).

[12] W. G. Noid, J.-W. Chu, G. S. Ayton, and G. A. Voth, J. Phys. Chem. B **111**, 4116 (2007).

[13] D. van der Spoel, E. Lindahl, B. Hess, A. R. van Buuren, E. Apol, P. J. Meulenhoff, D. P. Tieleman, A. L. T. M. Sijbers, K. A. Feenstra, R. van Drunen, et al., Gromacs user manual version 3.3 (2005).

[14] E. Anderson, Z. Bai, C. Bischof, S. Blackford, J. Demmel, J. Dongarra, J. D. Croz, A. Greenbaum, S. Hammarling, A. McKenney, et al., LAPACK Users' Guide (SIAM, 1999).

[15] W. H. Press, S. A. Teukolsky, W. T. Vetterling, and B. P. Flannery, Numerical Recipes in FORTRAN: The art of scientific computing (Cambridge University Press, 1992).

[16] J. W. Demmel, Applied Numerical Linear Algebra (SIAM, 1997).

II. SUPPLEMENTAL FIGURES

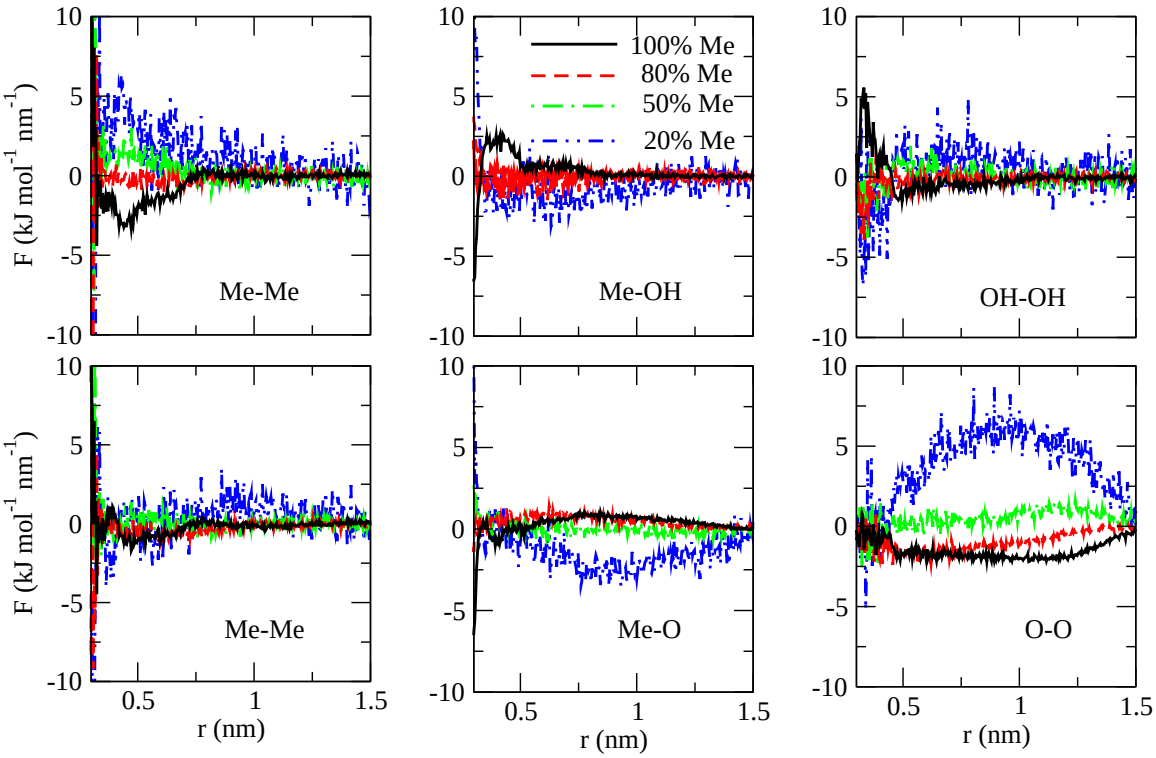

FIG. 1: Differences between the MS-CG pair forces calculated separately for topologies in the M2N1 and M3N1 ensembles and the optimal transferable pair forces presented in Fig. 5 of the manuscript. The top row presents the differences for the Me-Me, Me-OH, and OH-OH pair forces, respectively, calculated for the M2N1 extended ensemble. The bottom row presents the differences for the Me-Me, Me-O, and O-O pair forces, respectively, calculated for the M3N1 extended ensemble. In these panels, black, red, green, and blue curves correspond to binary methanol:neopentane mixtures with 100%, 80%, 50%, and 20% methanol, respectively.

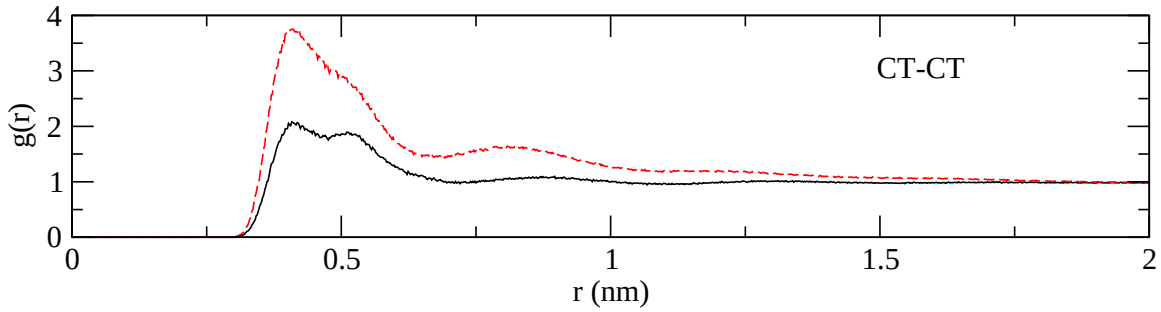

FIG. 2: Comparison of atomistic and CG site-site RDFs for the mixture of 544 ethanol and 136 ethane molecules used in parameterizing the transferable CG potential functions. RDFs calculated from atomistic and CG MD simulations are presented as the solid black and dashed red curves, respectively. In each case, the sites in each pair are from distinct ethane molecules.

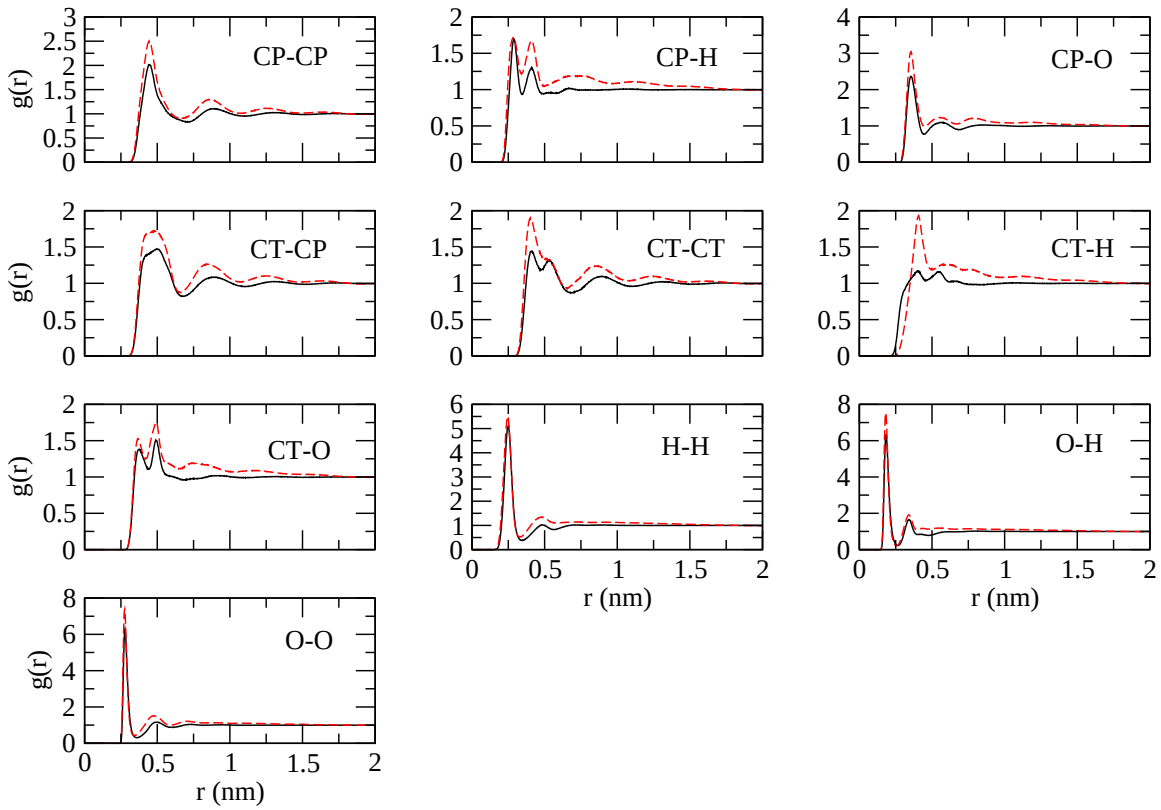

FIG. 3: Comparison of atomistic and CG site-site RDFs for the mixture of 544 ethanol and 136 ethane molecules used in parameterizing the transferable CG potential functions. RDFs calculated from atomistic and CG MD simulations are presented as the solid black and dashed red curves, respectively. In each case, the sites in each pair are from distinct ethanol molecules.

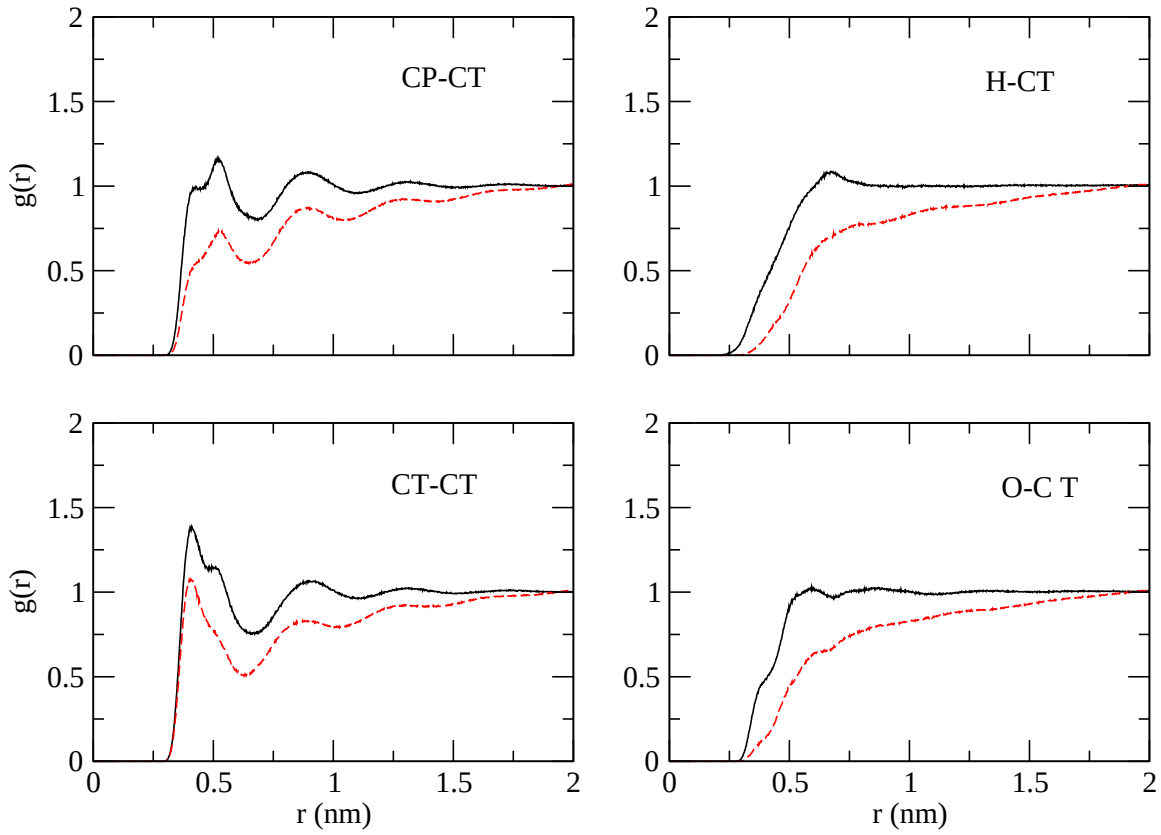

FIG. 4: Comparison of atomistic and CG site-site RDFs for the mixture of 544 ethanol and 136 ethane molecules used in parameterizing the transferable CG potential functions. RDFs calculated from atomistic and CG MD simulations are presented as the solid black and dashed red curves, respectively. In each case, the first and second sites in each pair are from distinct ethanol and ethane molecules, respectively.

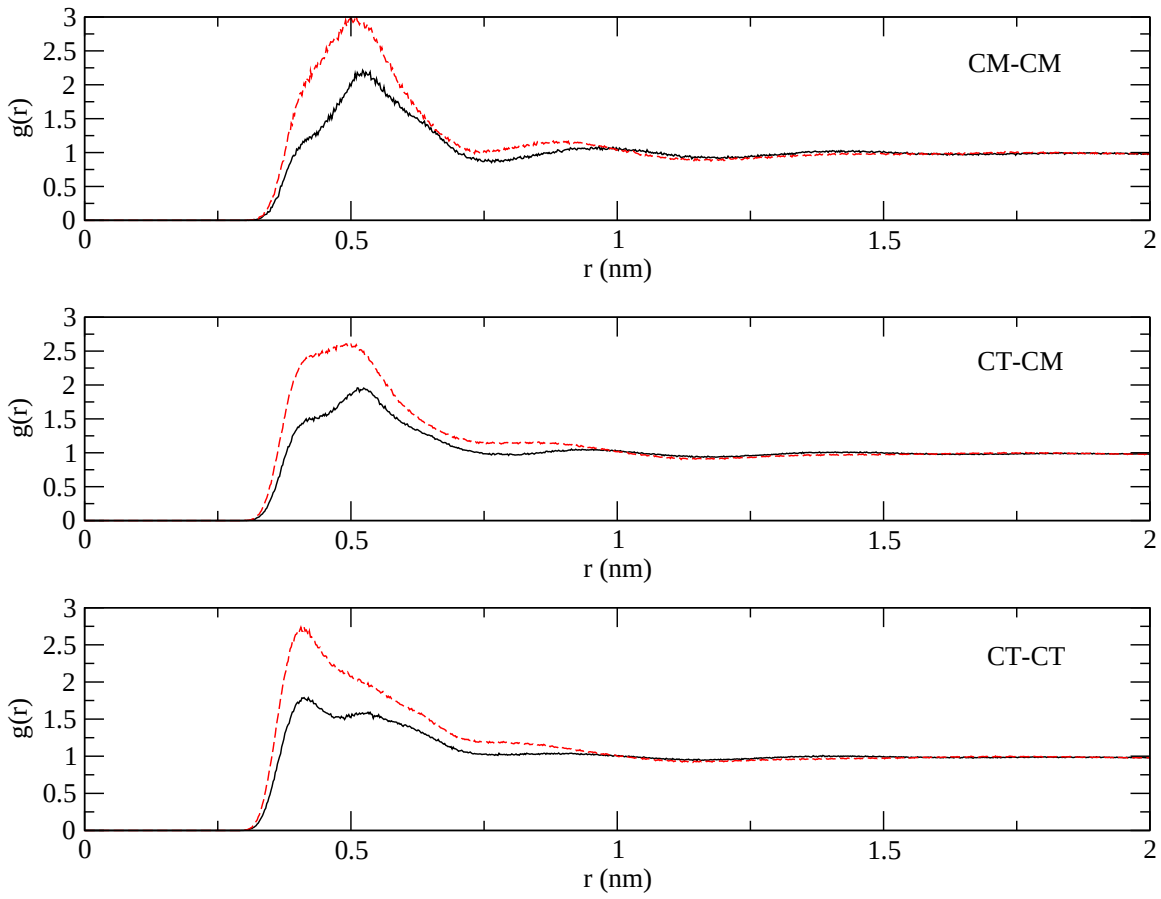

FIG. 5: Comparison of atomistic and CG site-site RDFs for the mixture of 416 propanol and 104 propane molecules used in parameterizing the transferable CG potential functions. RDFs calculated from atomistic and CG MD simulations are presented as the solid black and dashed red curves, respectively. In each case, the sites in each pair are from distinct propane molecules.

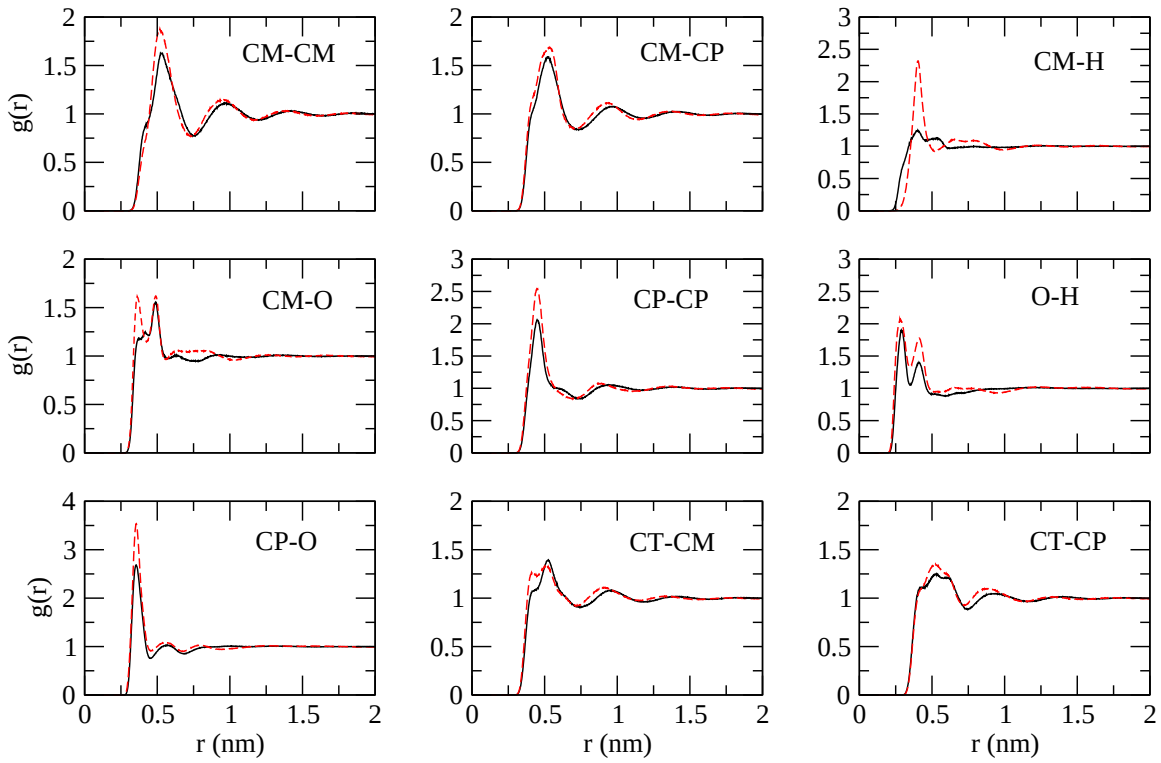

FIG. 6: Comparison of atomistic and CG site-site RDFs for the mixture of 416 propanol and 104 propane molecules used in parameterizing the transferable CG potential functions. RDFs calculated from atomistic and CG MD simulations are presented as the solid black and dashed red curves, respectively. In each case, the sites in each pair are from distinct propanol molecules.

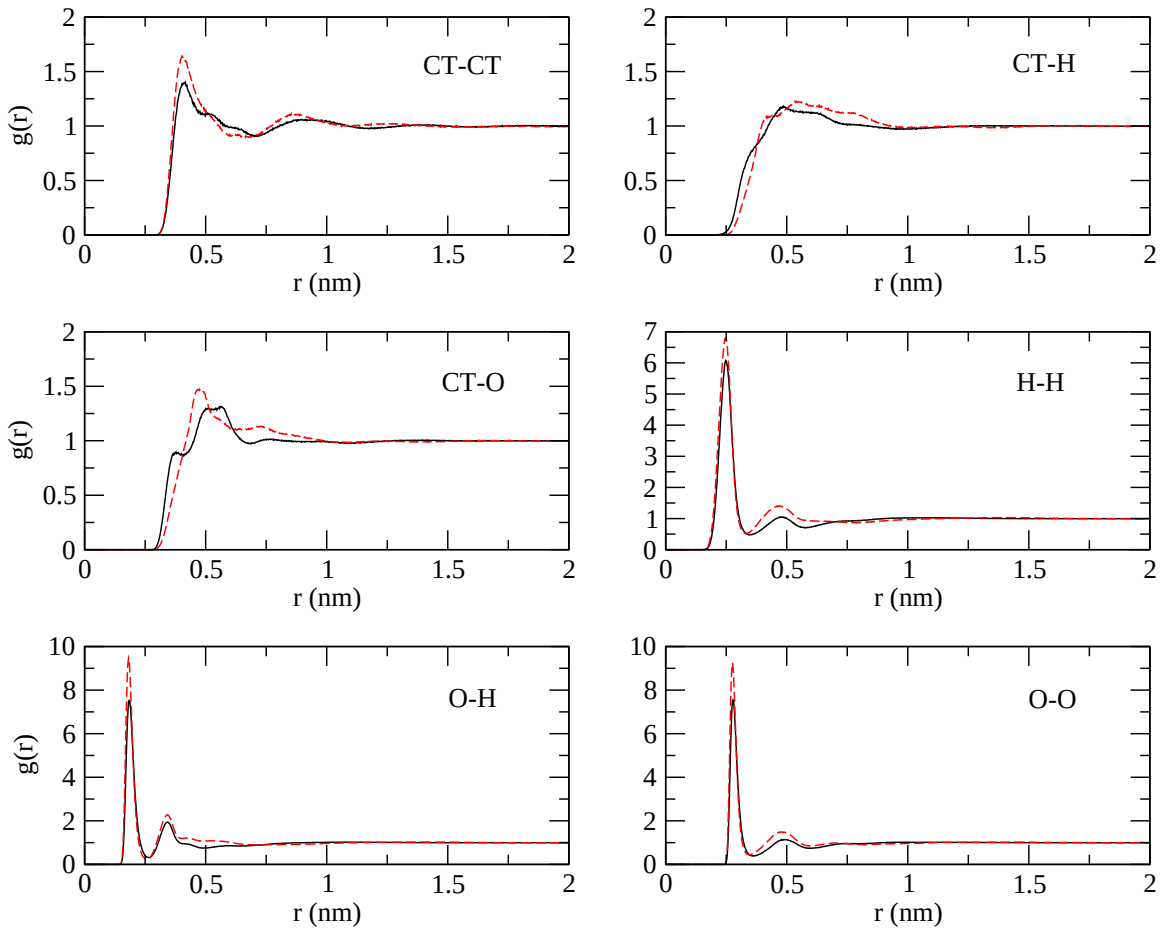

FIG. 7: Comparison of atomistic and CG site-site RDFs for the mixture of 416 propanol and 104 propane molecules used in parameterizing the transferable CG potential functions. RDFs calculated from atomistic and CG MD simulations are presented as the solid black and dashed red curves, respectively. In each case, the sites in each pair are from distinct propanol molecules.

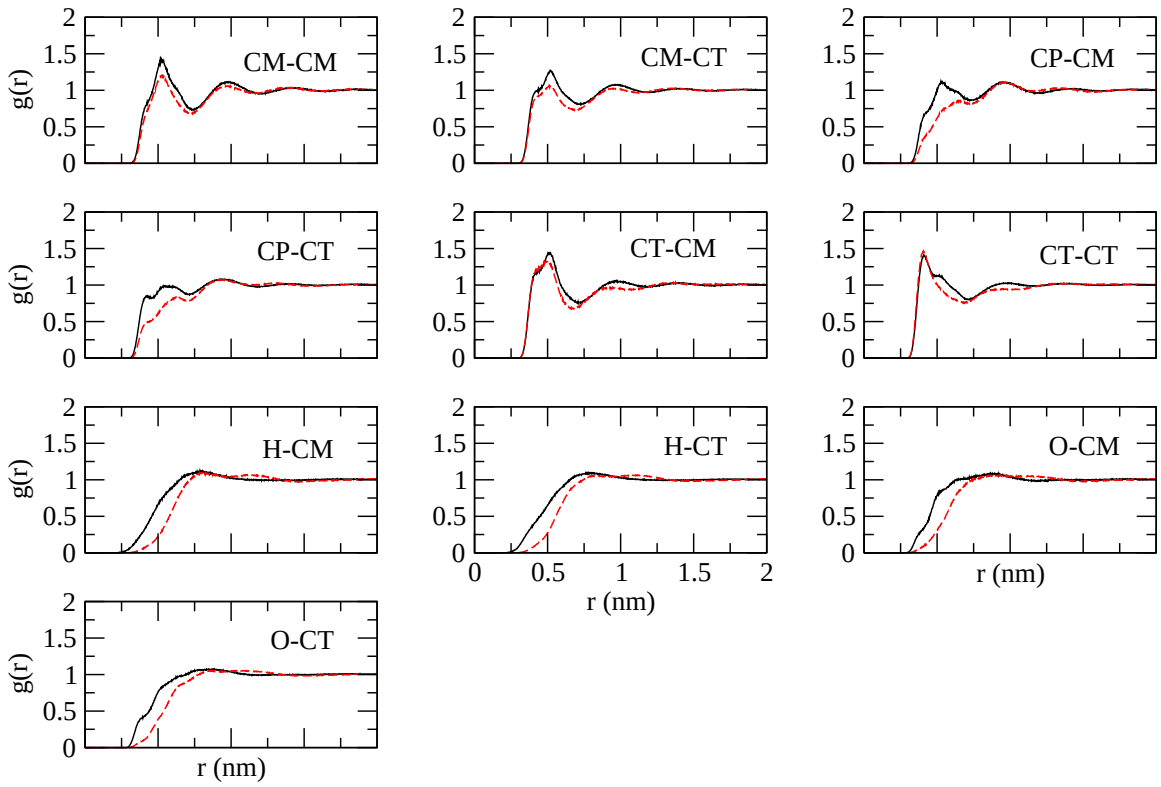

FIG. 8: Comparison of atomistic and CG site-site RDFs for the mixture of 416 propanol and 104 propane molecules used in parameterizing the transferable CG potential functions. RDFs calculated from atomistic and CG MD simulations are presented as the solid black and dashed red curves, respectively. In each case, the first and second sites in each pair are from distinct propanol and propane molecules, respectively.

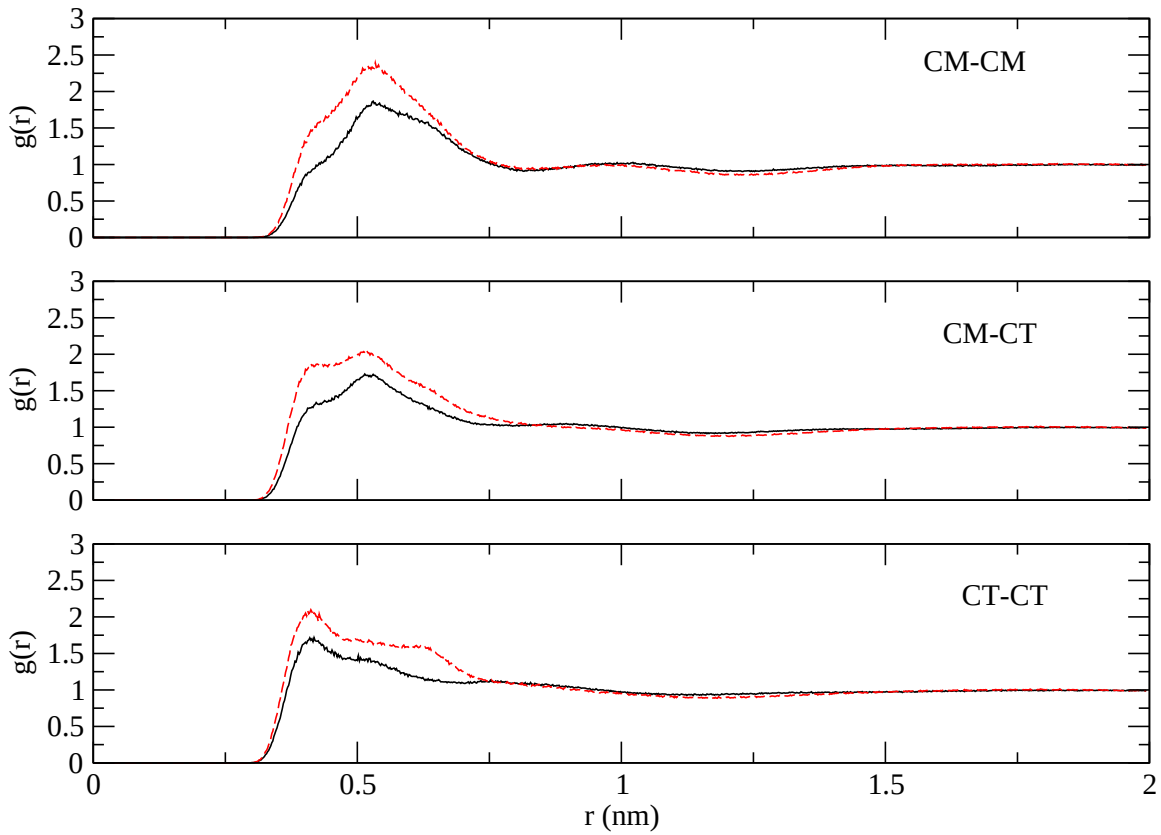

FIG. 9: Comparison of atomistic and CG site-site RDFs for the mixture of 336 butanol and 84 butane molecules used in parameterizing the transferable CG potential functions. RDFs calculated from atomistic and CG MD simulations are presented as the solid black and dashed red curves, respectively. In each case, the sites in each pair are from distinct butane molecules.

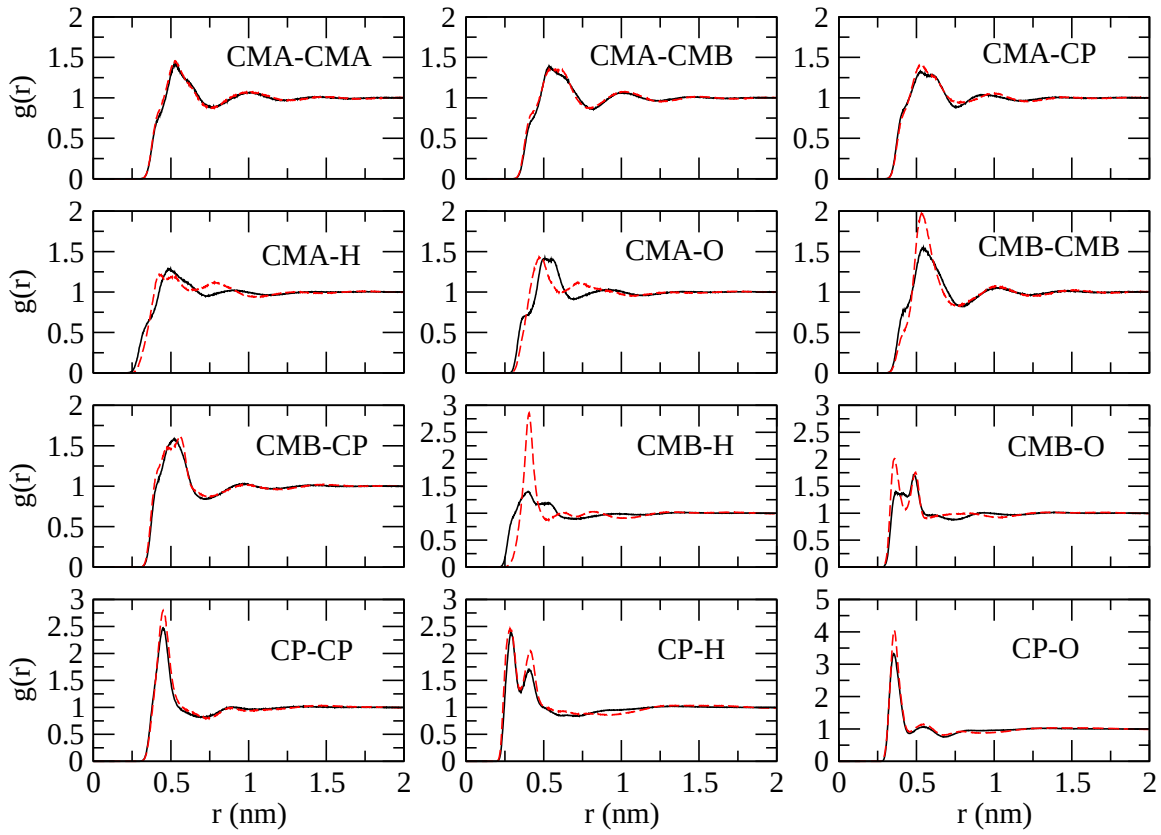

FIG. 10: Comparison of atomistic and CG site-site RDFs for the mixture of 336 butanol and 84 butane molecules used in parameterizing the transferable CG potential functions. RDFs calculated from atomistic and CG MD simulations are presented as the solid black and dashed red curves, respectively. In each case, the sites in each pair are from distinct butanol molecules. CMA refers to the CM site next to the CT site in butanol, and CMB refers to the CM site next to the CP site in butanol.

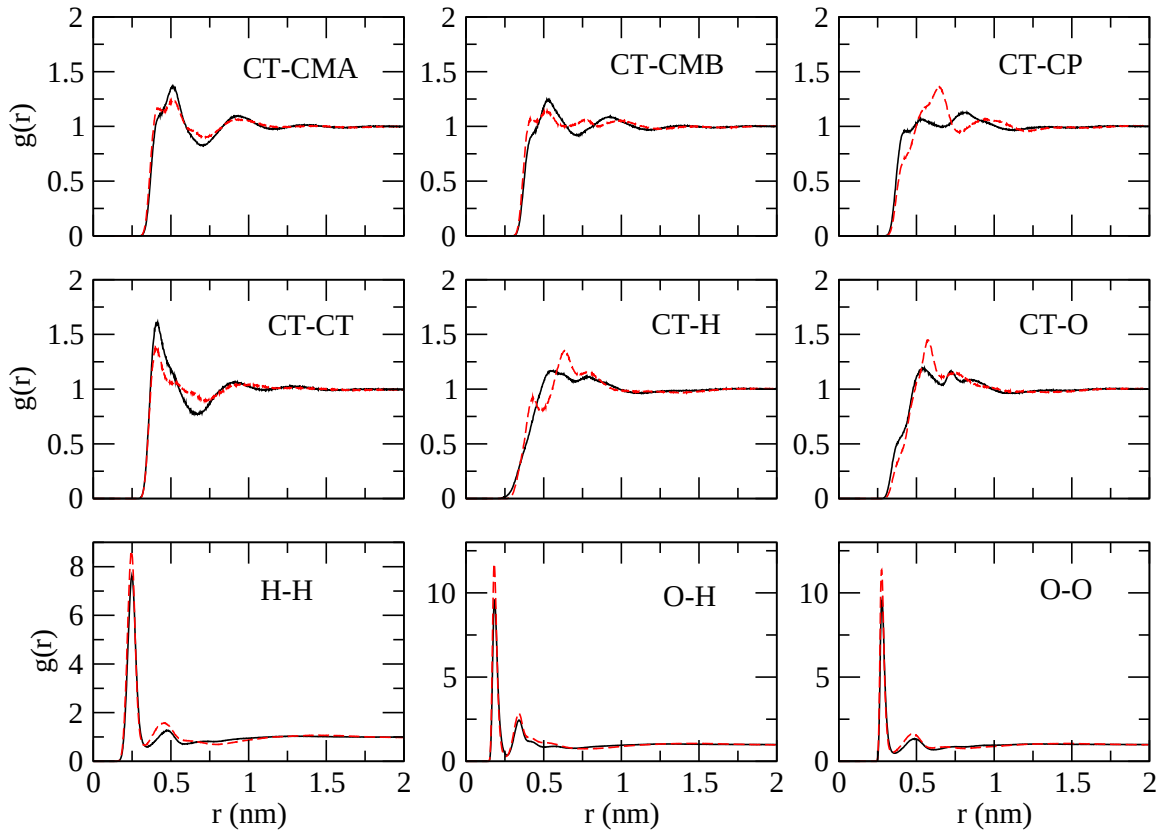

FIG. 11: Comparison of atomistic and CG site-site RDFs for the mixture of 336 butanol and 84 butane molecules used in parameterizing the transferable CG potential functions. RDFs calculated from atomistic and CG MD simulations are presented as the solid black and dashed red curves, respectively. In each case, the sites in each pair are from distinct butanol molecules. CMA refers to the CM site next to the CT site in butanol, and CMB refers to the CM site next to the CP site in butanol.

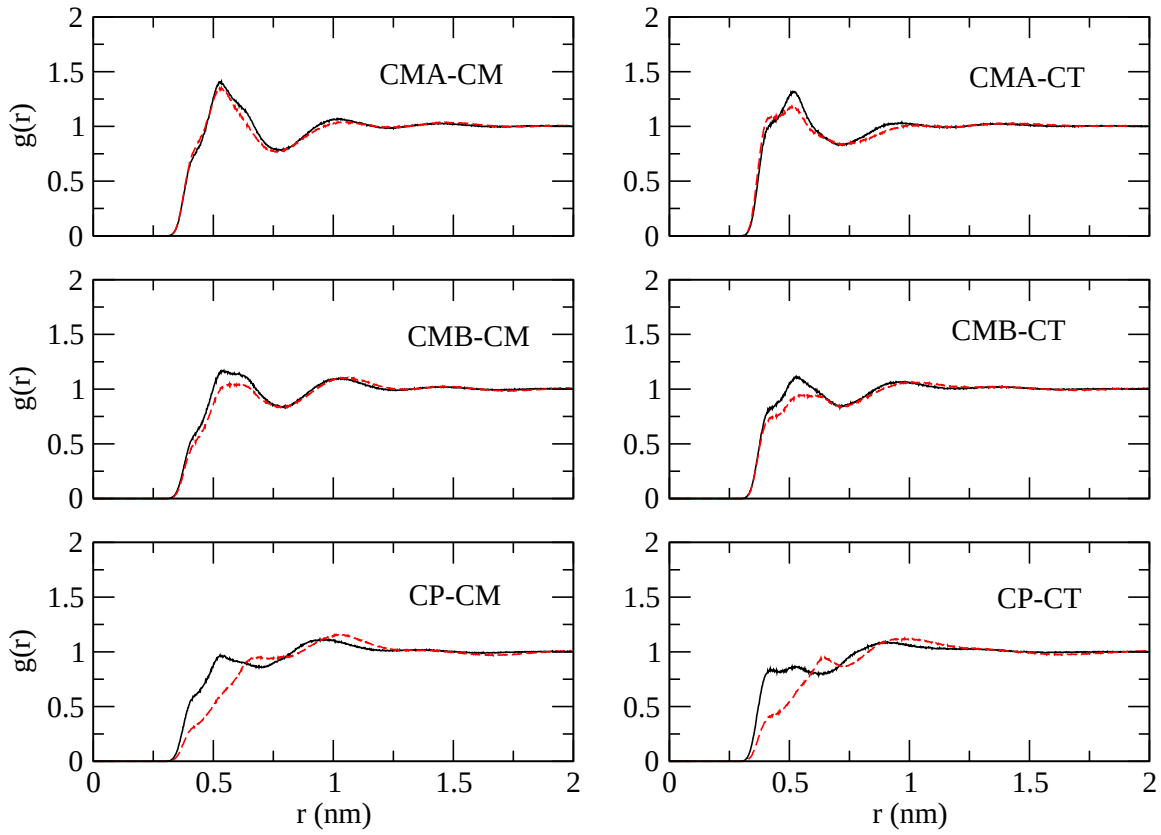

FIG. 12: Comparison of atomistic and CG site-site RDFs for the mixture of 336 butanol and 84 butane molecules used in parameterizing the transferable CG potential functions. RDFs calculated from atomistic and CG MD simulations are presented as the solid black and dashed red curves, respectively. In each case, the first and second sites in each pair are from distinct butanol and butane molecules, respectively. CMA refers to the CM site next to the CT site in butanol, and CMB refers to the CM site next to the CP site in butanol.

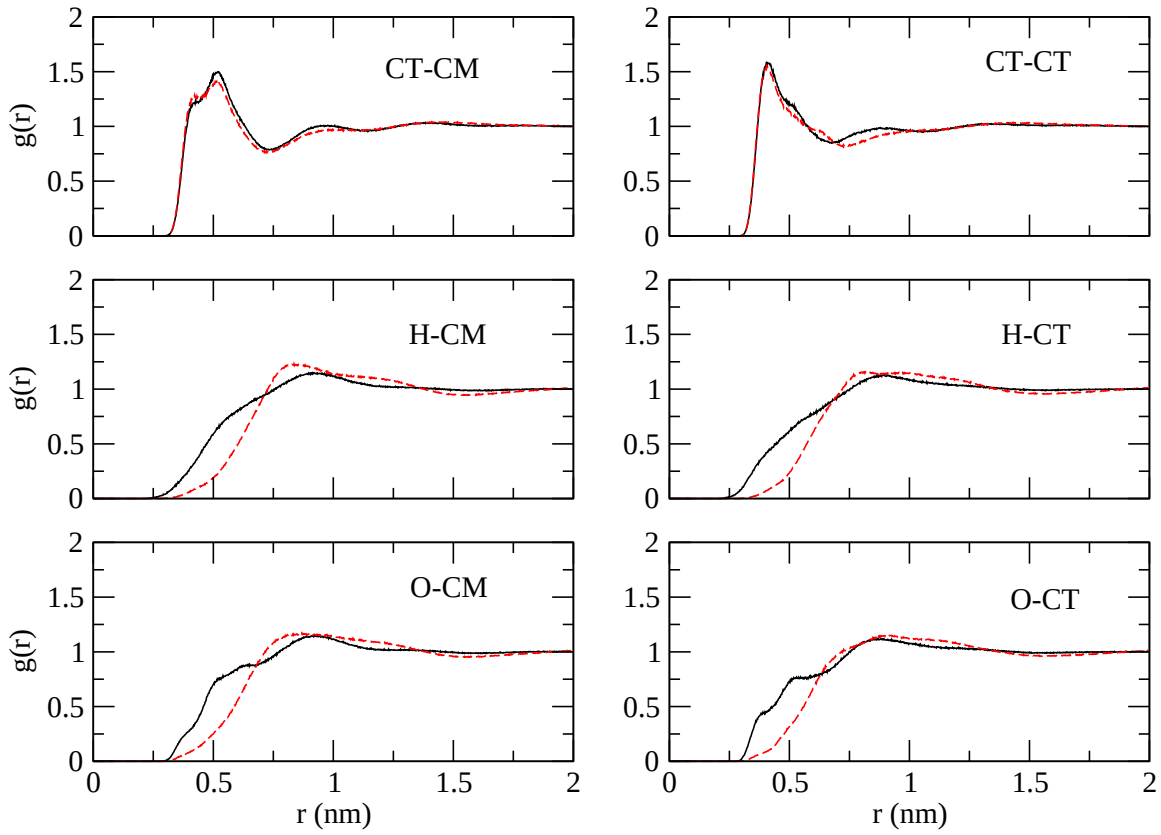

FIG. 13: Comparison of atomistic and CG site-site RDFs for the mixture of 336 butanol and 84 butane molecules used in parameterizing the transferable CG potential functions. RDFs calculated from atomistic and CG MD simulations are presented as the solid black and dashed red curves, respectively. In each case, the first and second sites in each pair are from distinct butanol and butane molecules, respectively. CMA refers to the CM site next to the CT site in butanol, and CMB refers to the CM site next to the CP site in butanol.

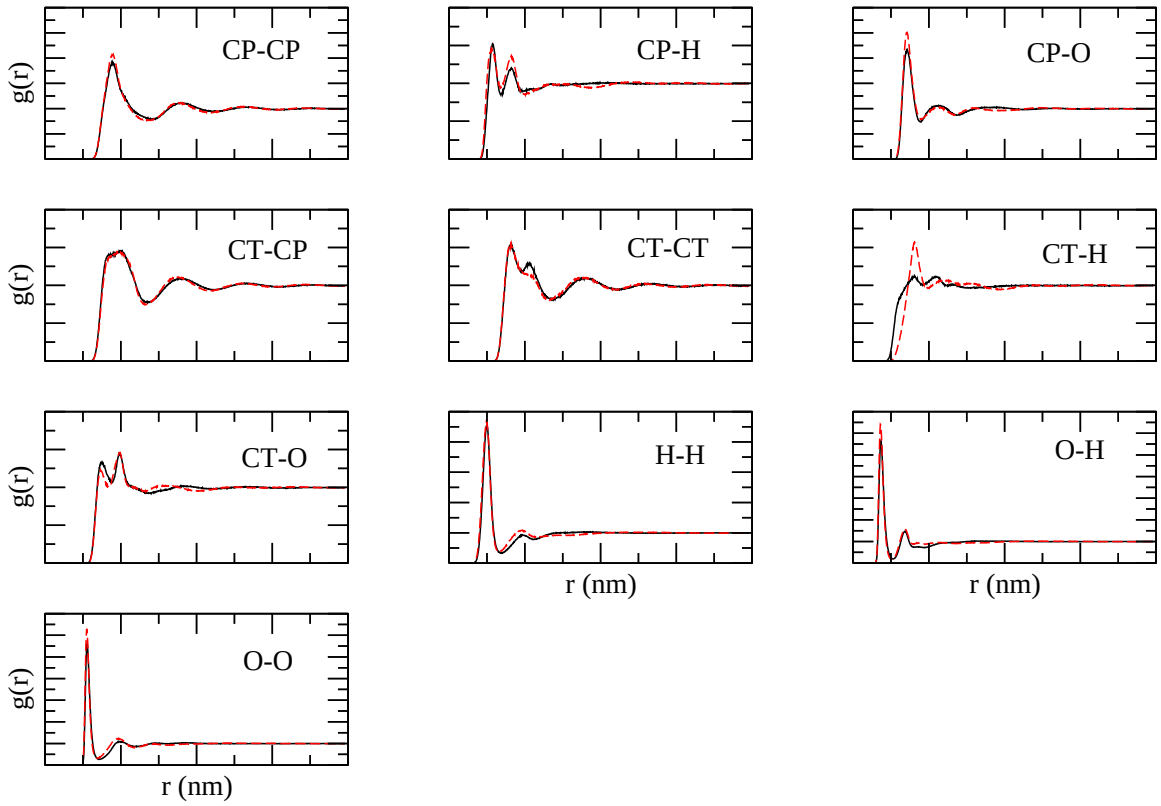

FIG. 14: Comparison of atomistic and CG site-site RDFs for the mixture of 290 ethanol and 290 propanol molecules used in parameterizing the transferable CG potential functions. RDFs calculated from atomistic and CG MD simulations are presented as the solid black and dashed red curves, respectively. In each case, the sites in each pair are from distinct ethanol molecules.

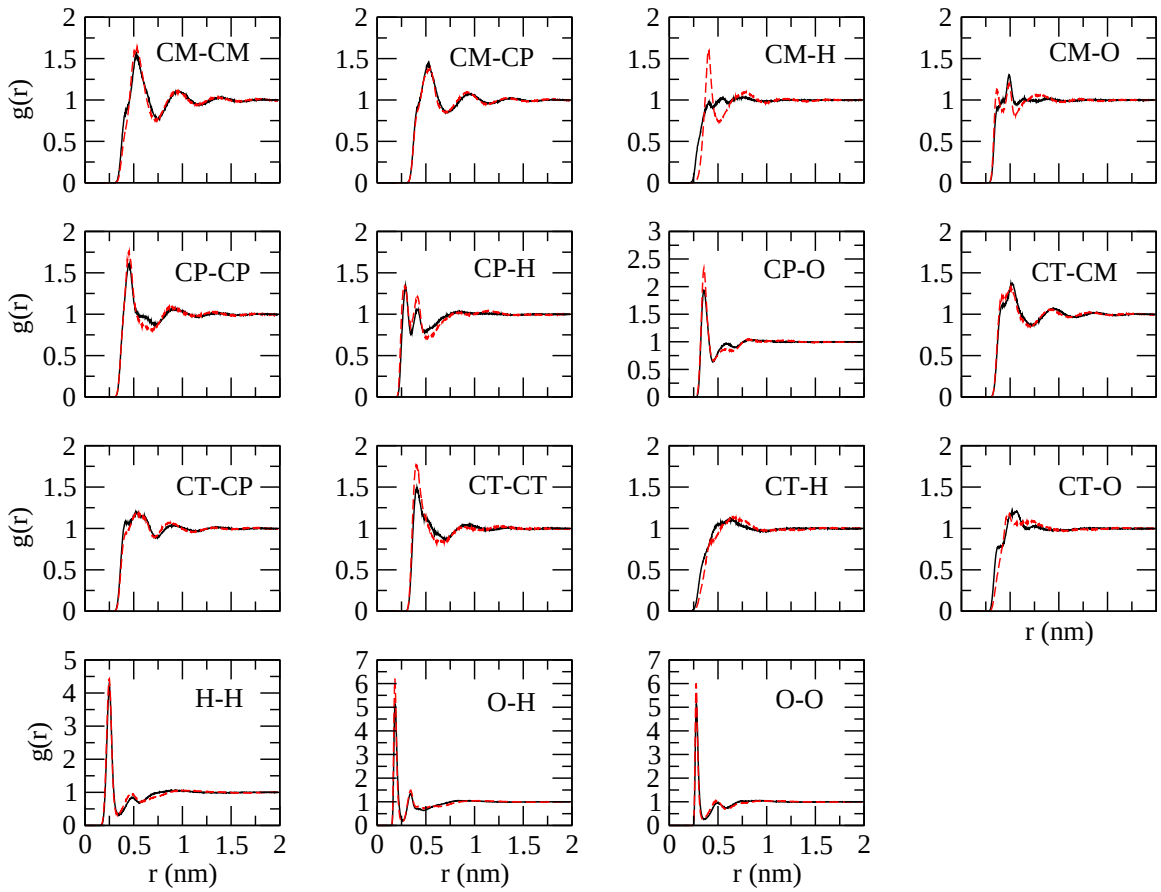

FIG. 15: Comparison of atomistic and CG site-site RDFs for the mixture of 290 ethanol and 290 propanol molecules used in parameterizing the transferable CG potential functions. RDFs calculated from atomistic and CG MD simulations are presented as the solid black and dashed red curves, respectively. In each case, the sites in each pair are from distinct propanol molecules.

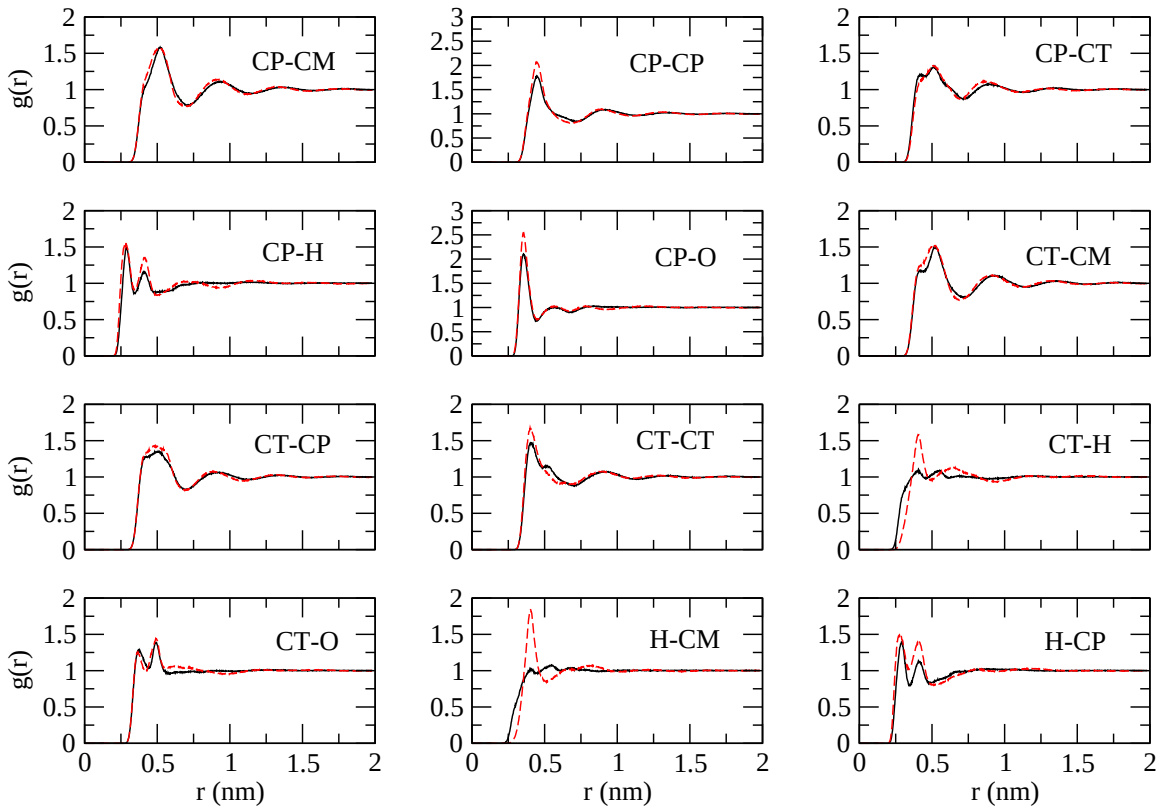

FIG. 16: Comparison of atomistic and CG site-site RDFs for the mixture of 290 ethanol and 290 propanol molecules used in parameterizing the transferable CG potential functions. RDFs calculated from atomistic and CG MD simulations are presented as the solid black and dashed red curves, respectively. In each case, the first and second sites in each pair are from distinct ethanol and propanol molecules, respectively.

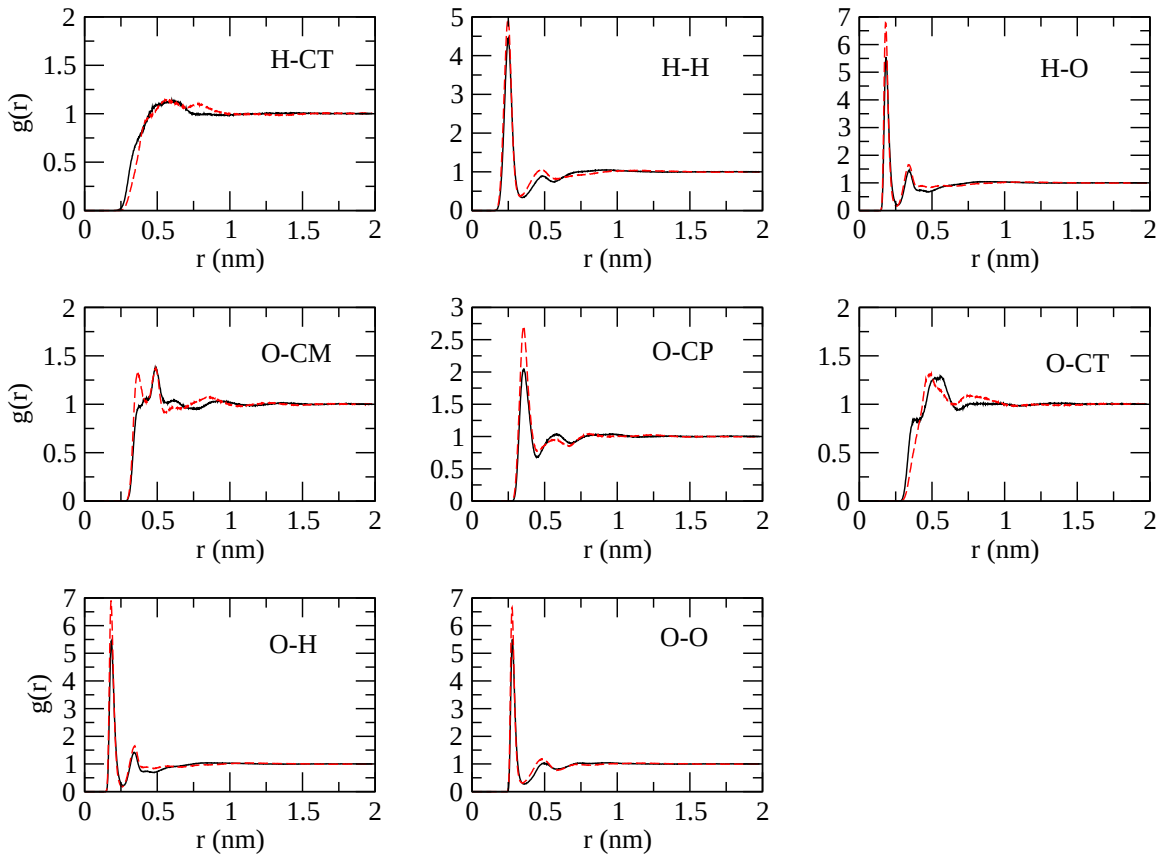

FIG. 17: Comparison of atomistic and CG site-site RDFs for the mixture of 290 ethanol and 290 propanol molecules used in parameterizing the transferable CG potential functions. RDFs calculated from atomistic and CG MD simulations are presented as the solid black and dashed red curves, respectively. In each case, the first and second sites in each pair are from distinct ethanol and propanol molecules, respectively.

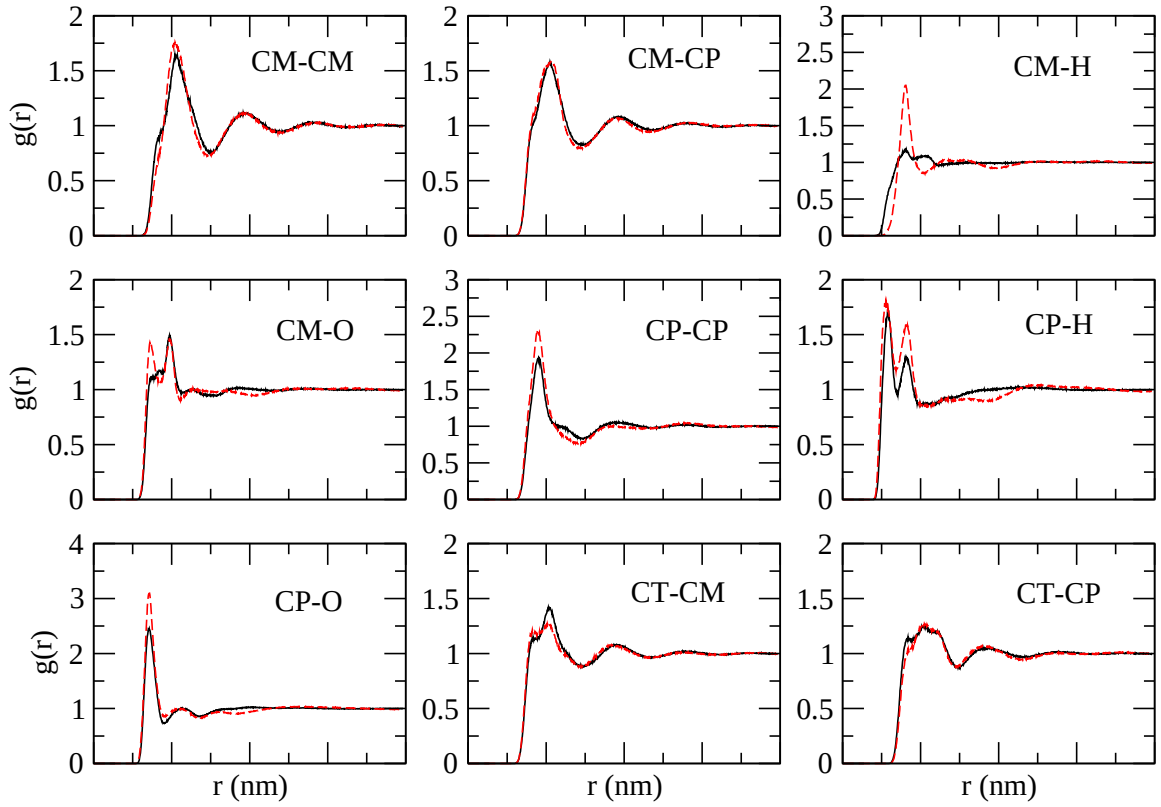

FIG. 18: Comparison of atomistic and CG site-site RDFs for the mixture of 232 propanol and 232 butanol molecules used in parameterizing the transferable CG potential functions. RDFs calculated from atomistic and CG MD simulations are presented as the solid black and dashed red curves, respectively. In each case, the sites in each pair are from distinct propanol molecules.

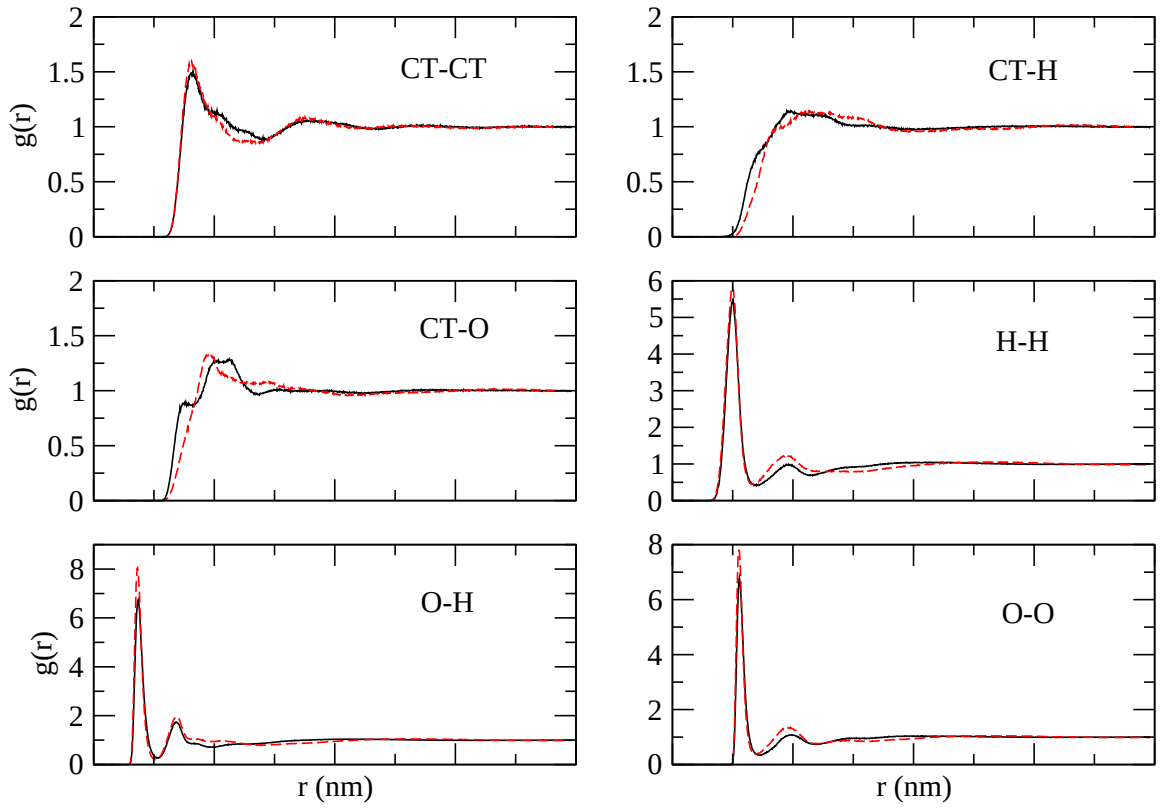

FIG. 19: Comparison of atomistic and CG site-site RDFs for the mixture of 232 propanol and 232 butanol molecules used in parameterizing the transferable CG potential functions. RDFs calculated from atomistic and CG MD simulations are presented as the solid black and dashed red curves, respectively. In each case, the sites in each pair are from distinct propanol molecules.

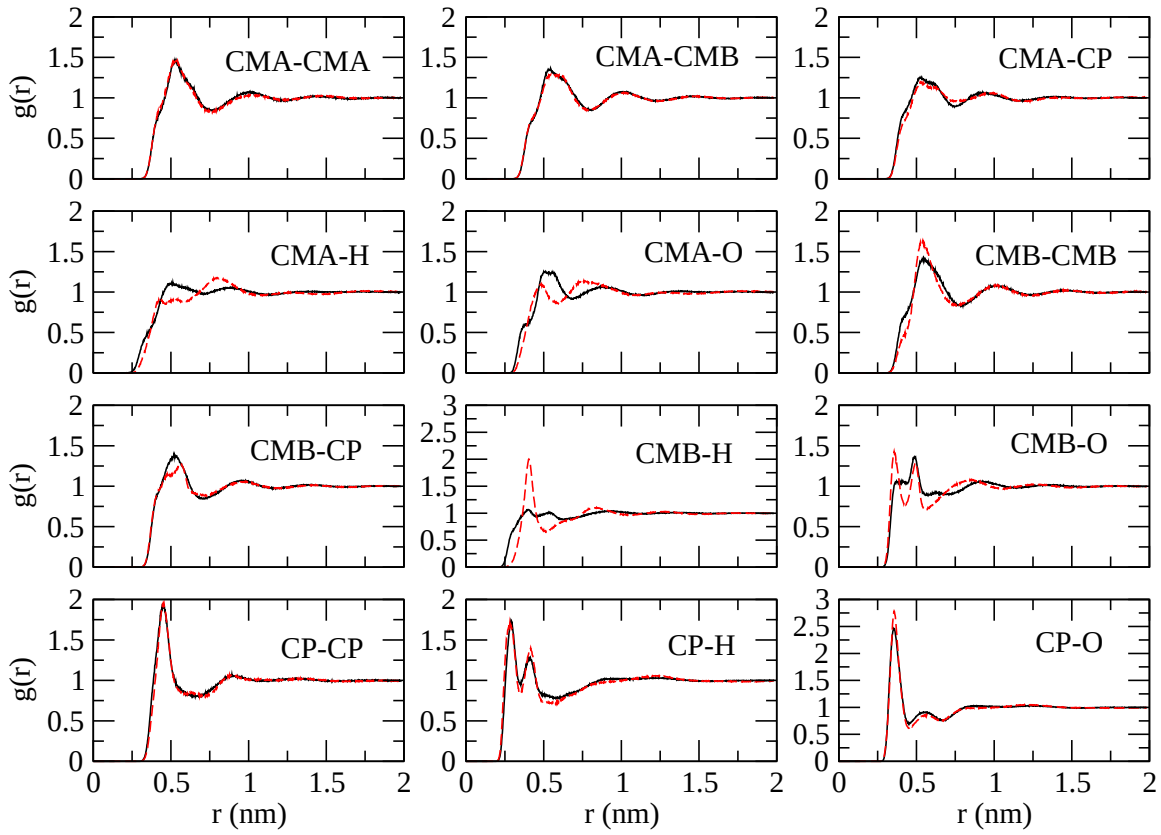

FIG. 20: Comparison of atomistic and CG site-site RDFs for the mixture of 232 propanol and 232 butanol molecules used in parameterizing the transferable CG potential functions. RDFs calculated from atomistic and CG MD simulations are presented as the solid black and dashed red curves, respectively. In each case, the sites in each pair are from distinct butanol molecules. CMA refers to the CM site next to the CT site in butanol, and CMB refers to the CM site next to the CP site in butanol.

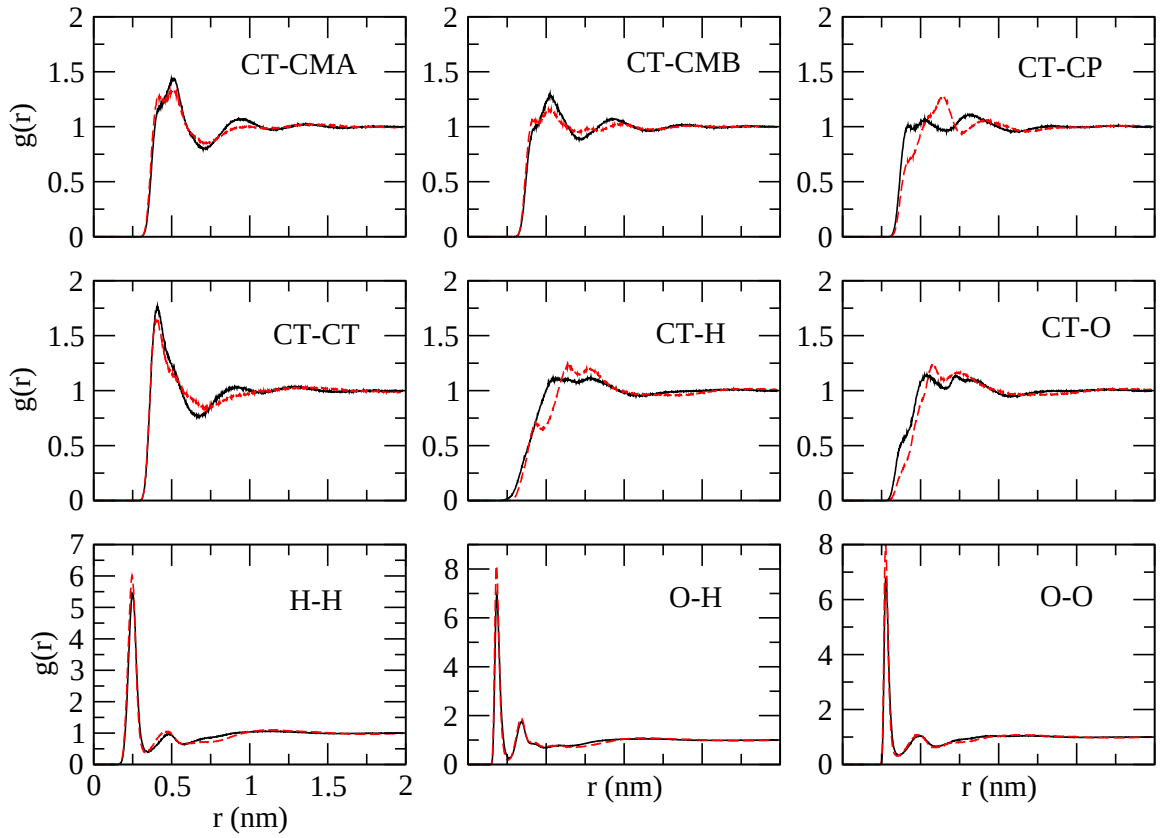

FIG. 21: Comparison of atomistic and CG site-site RDFs for the mixture of 232 propanol and 232 butanol molecules used in parameterizing the transferable CG potential functions. RDFs calculated from atomistic and CG MD simulations are presented as the solid black and dashed red curves, respectively. In each case, the sites in each pair are from distinct butanol molecules. CMA refers to the CM site next to the CT site in butanol, and CMB refers to the CM site next to the CP site in butanol.

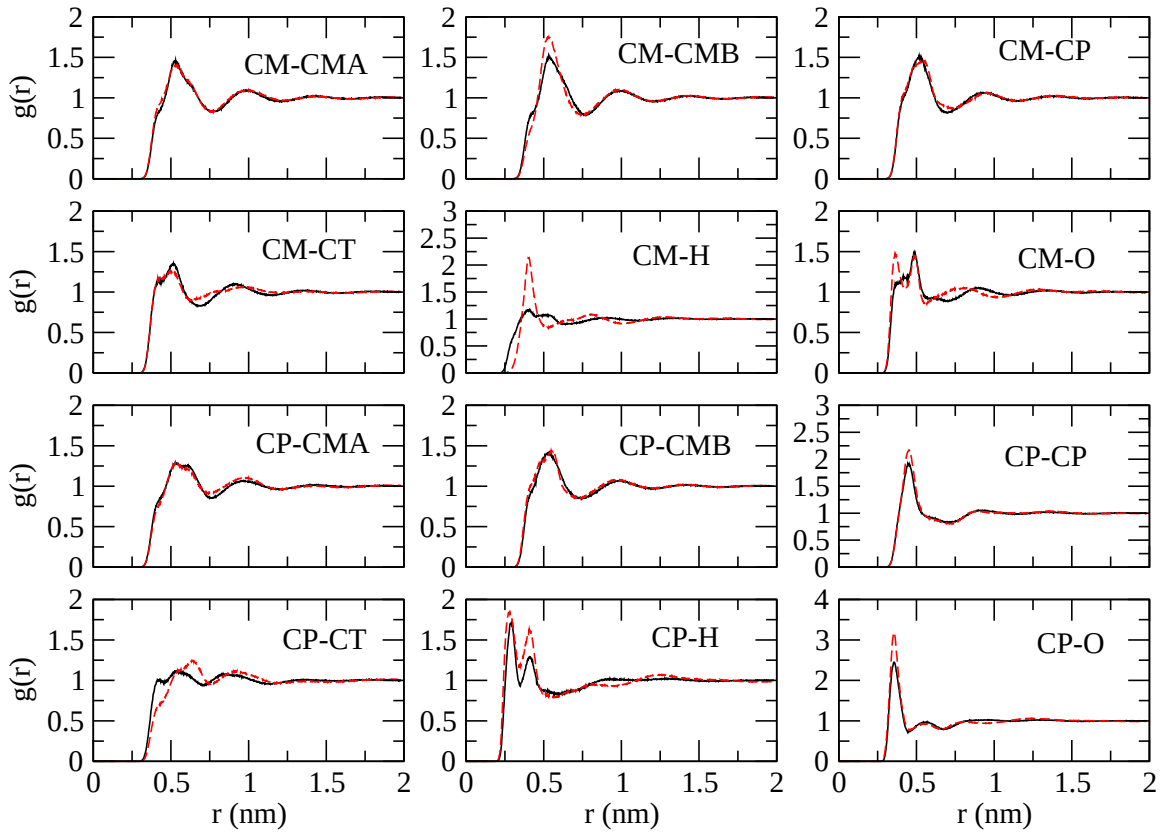

FIG. 22: Comparison of atomistic and CG site-site RDFs for the mixture of 232 propanol and 232 butanol molecules used in parameterizing the transferable CG potential functions. RDFs calculated from atomistic and CG MD simulations are presented as the solid black and dashed red curves, respectively. In each case, the first and second sites in each pair are from distinct propanol and butanol molecules, respectively. CMA refers to the CM site next to the CT site in butanol, and CMB refers to the CM site next to the CP site in butanol.

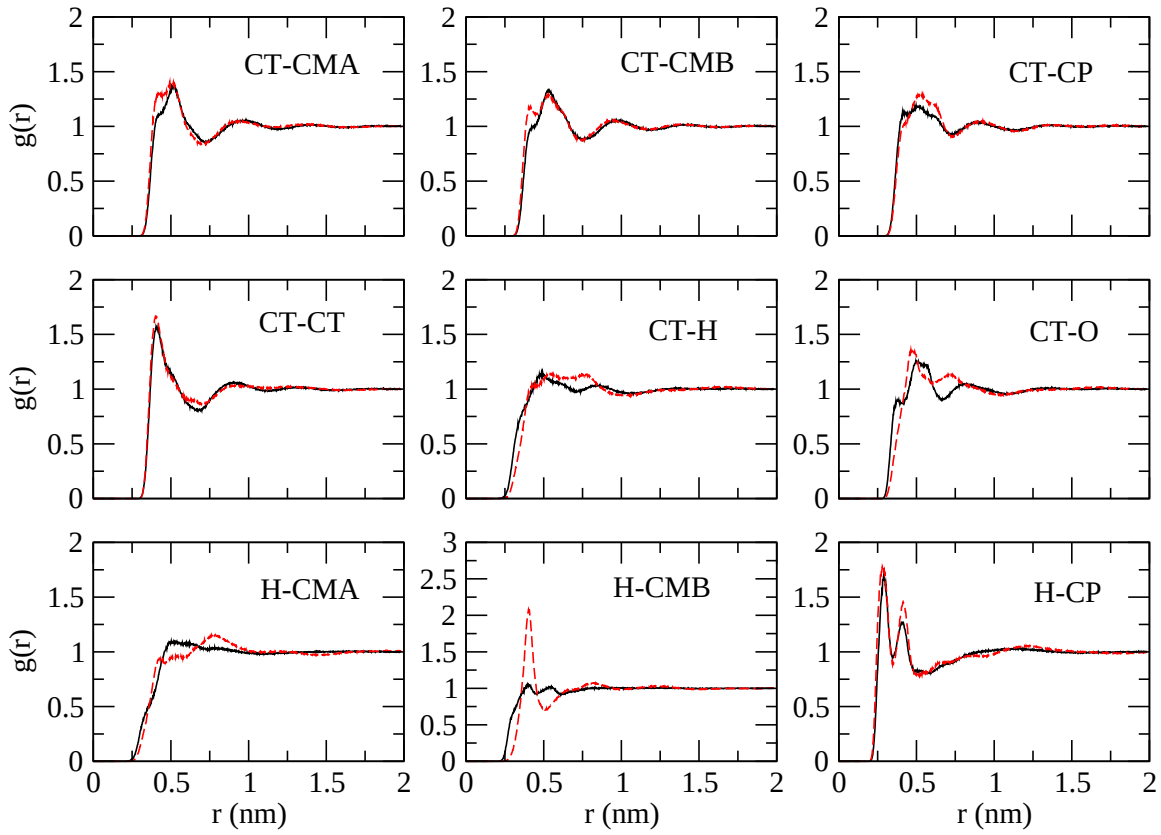

FIG. 23: Comparison of atomistic and CG site-site RDFs for the mixture of 232 propanol and 232 butanol molecules used in parameterizing the transferable CG potential functions. RDFs calculated from atomistic and CG MD simulations are presented as the solid black and dashed red curves, respectively. In each case, the first and second sites in each pair are from distinct propanol and butanol molecules, respectively. CMA refers to the CM site next to the CT site in butanol, and CMB refers to the CM site next to the CP site in butanol.

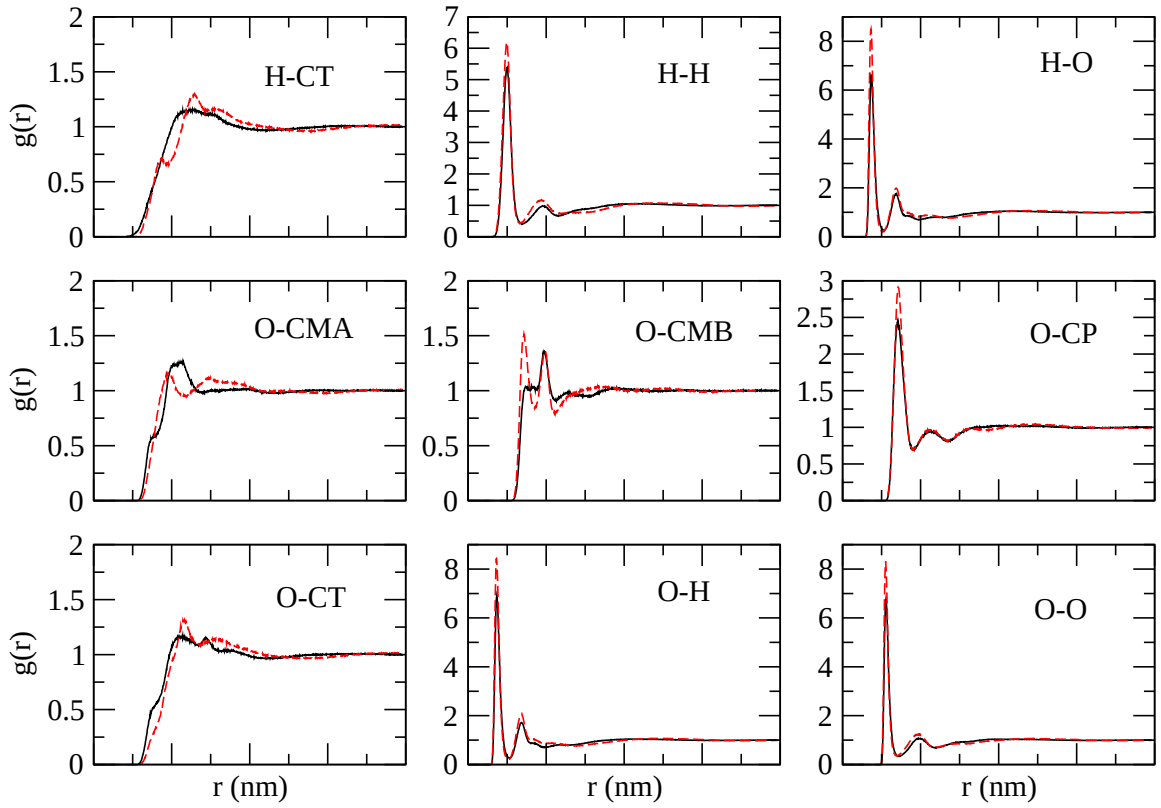

FIG. 24: Comparison of atomistic and CG site-site RDFs for the mixture of 232 propanol and 232 butanol molecules used in parameterizing the transferable CG potential functions. RDFs calculated from atomistic and CG MD simulations are presented as the solid black and dashed red curves, respectively. In each case, the first and second sites in each pair are from distinct propanol and butanol molecules, respectively. CMA refers to the CM site next to the CT site in butanol, and CMB refers to the CM site next to the CP site in butanol.

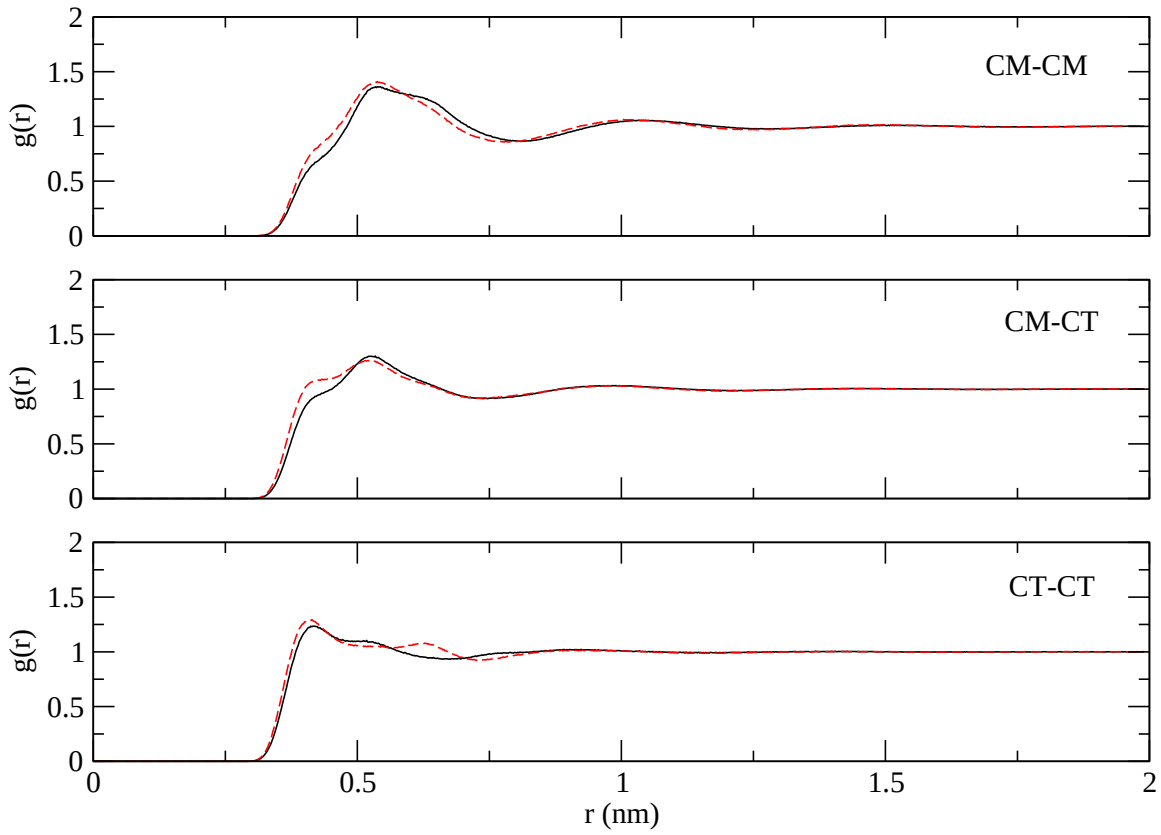

FIG. 25: Comparison of atomistic and CG site-site RDFs for the system of 380 butane molecules not used in parameterizing the transferable CG potential functions. RDFs calculated from atomistic and CG MD simulations are presented as the solid black and dashed red curves, respectively. In each case, the sites in each pair are from distinct butane molecules.

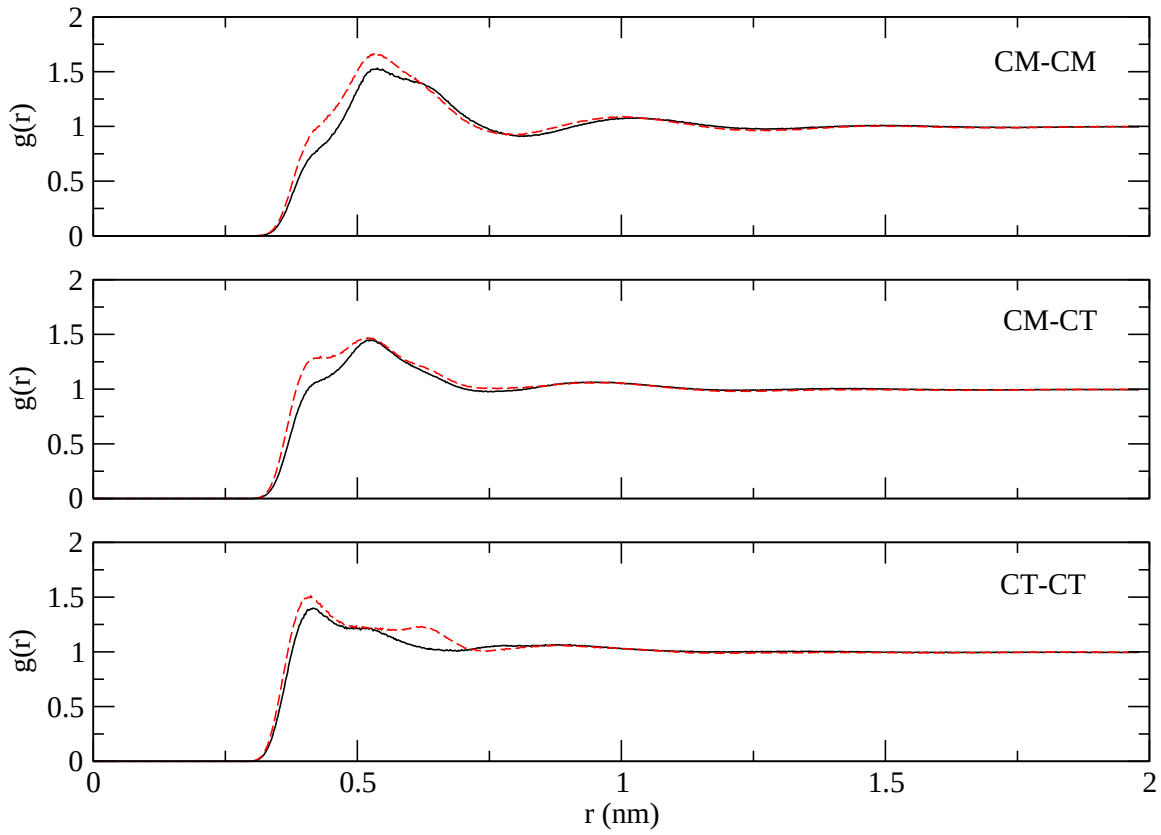

FIG. 26: Comparison of atomistic and CG site-site RDFs for the mixture of 130 butanol and 260 butane molecules not used in parameterizing the transferable CG potential functions. RDFs calculated from atomistic and CG MD simulations are presented as the solid black and dashed red curves, respectively. In each case, the sites in each pair are from distinct butane molecules.

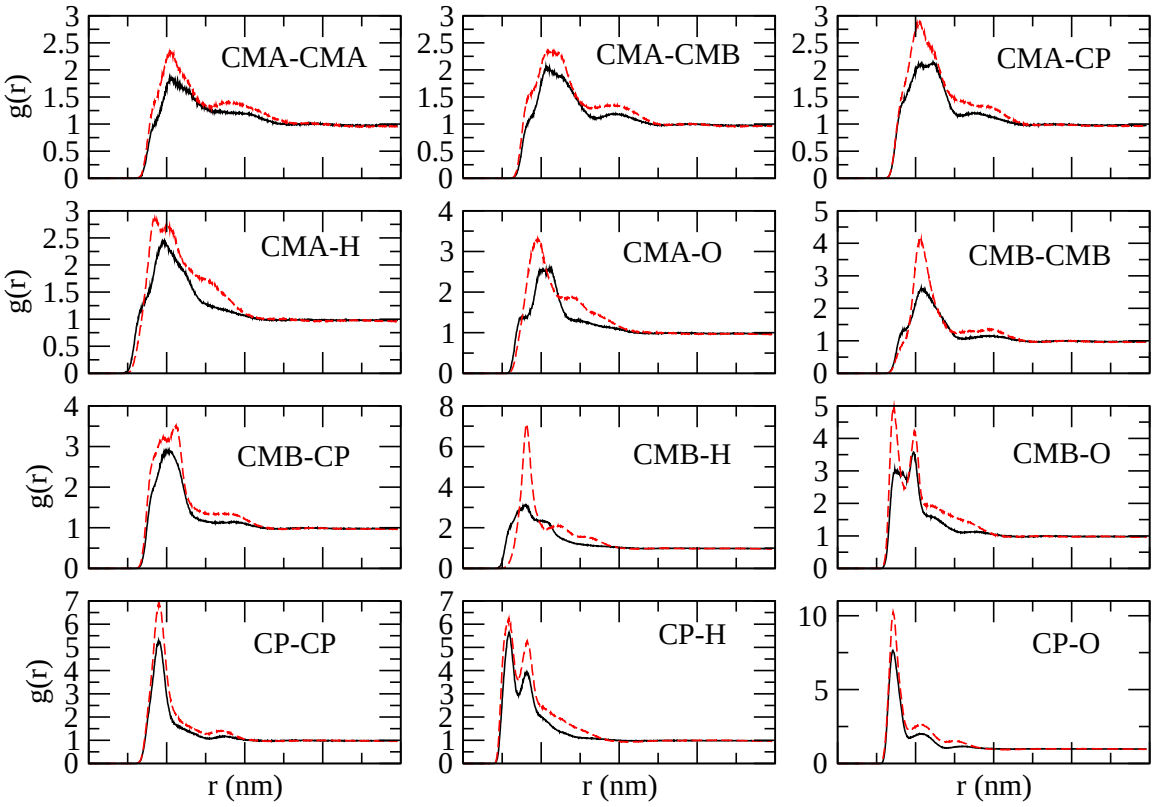

FIG. 27: Comparison of atomistic and CG site-site RDFs for the mixture of 130 butanol and 260 butane molecules not used in parameterizing the transferable CG potential functions. RDFs calculated from atomistic and CG MD simulations are presented as the solid black and dashed red curves, respectively. In each case, the sites in each pair are from distinct butanol molecules. CMA refers to the CM site next to the CT site in butanol, and CMB refers to the CM site next to the CP site in butanol.

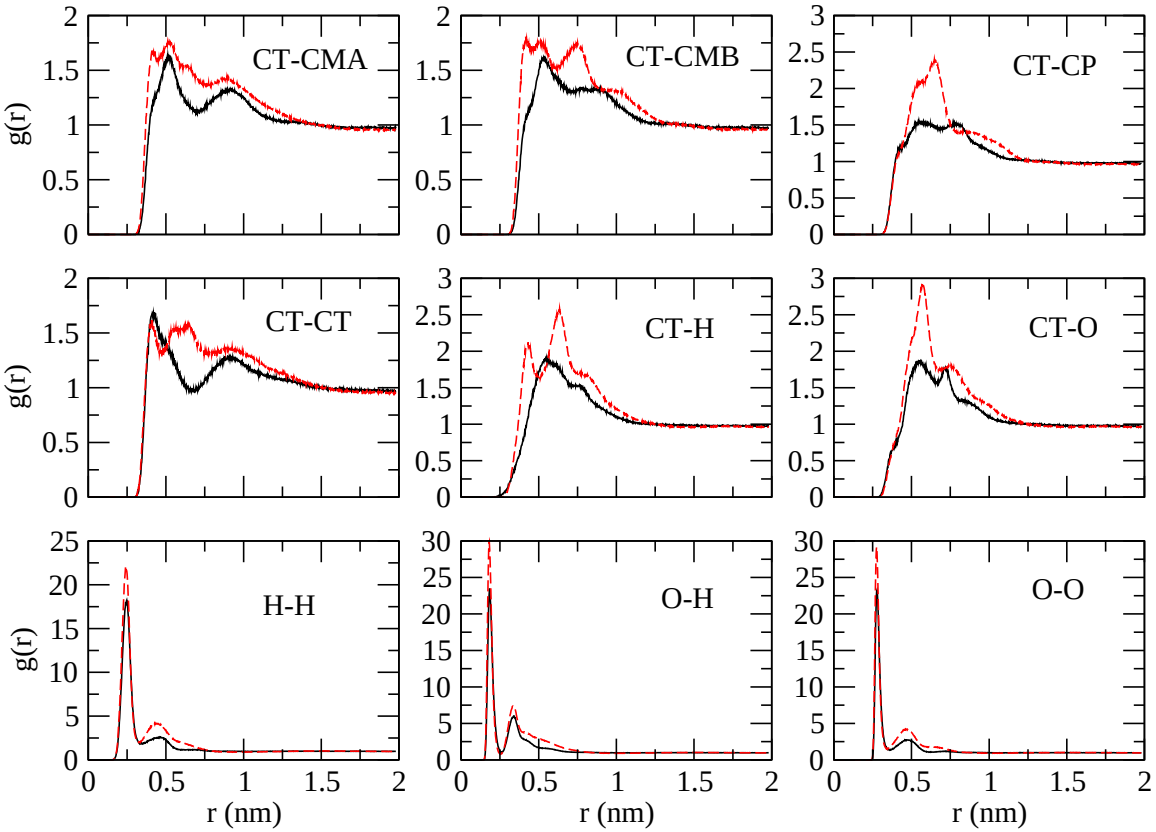

FIG. 28: Comparison of atomistic and CG site-site RDFs for the mixture of 130 butanol and 260 butane molecules not used in parameterizing the transferable CG potential functions. RDFs calculated from atomistic and CG MD simulations are presented as the solid black and dashed red curves, respectively. In each case, the sites in each pair are from distinct butanol molecules. CMA refers to the CM site next to the CT site in butanol, and CMB refers to the CM site next to the CP site in butanol.

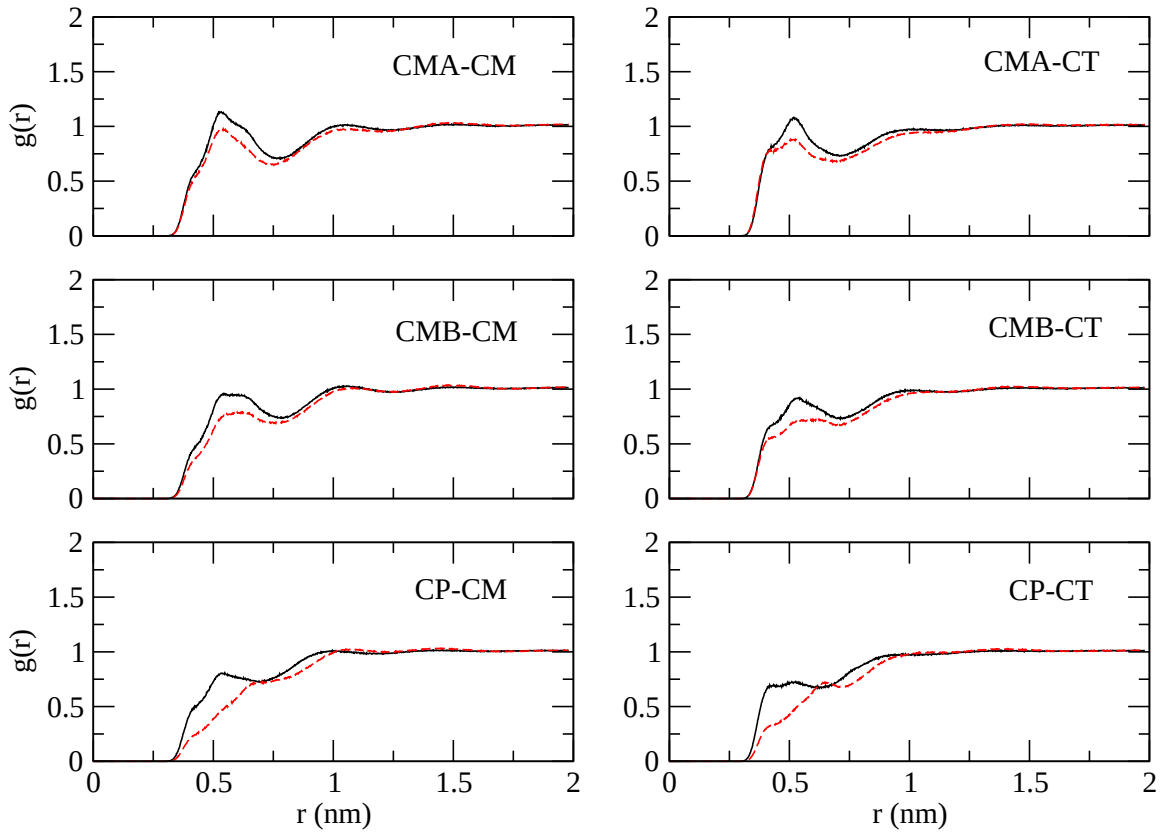

FIG. 29: Comparison of atomistic and CG site-site RDFs for the mixture of 130 butanol and 260 butane molecules not used in parameterizing the transferable CG potential functions. RDFs calculated from atomistic and CG MD simulations are presented as the solid black and dashed red curves, respectively. In each case, the first and second sites in each pair are from distinct butanol and butane molecules, respectively. CMA refers to the CM site next to the CT site in butanol, and CMB refers to the CM site next to the CP site in butanol.

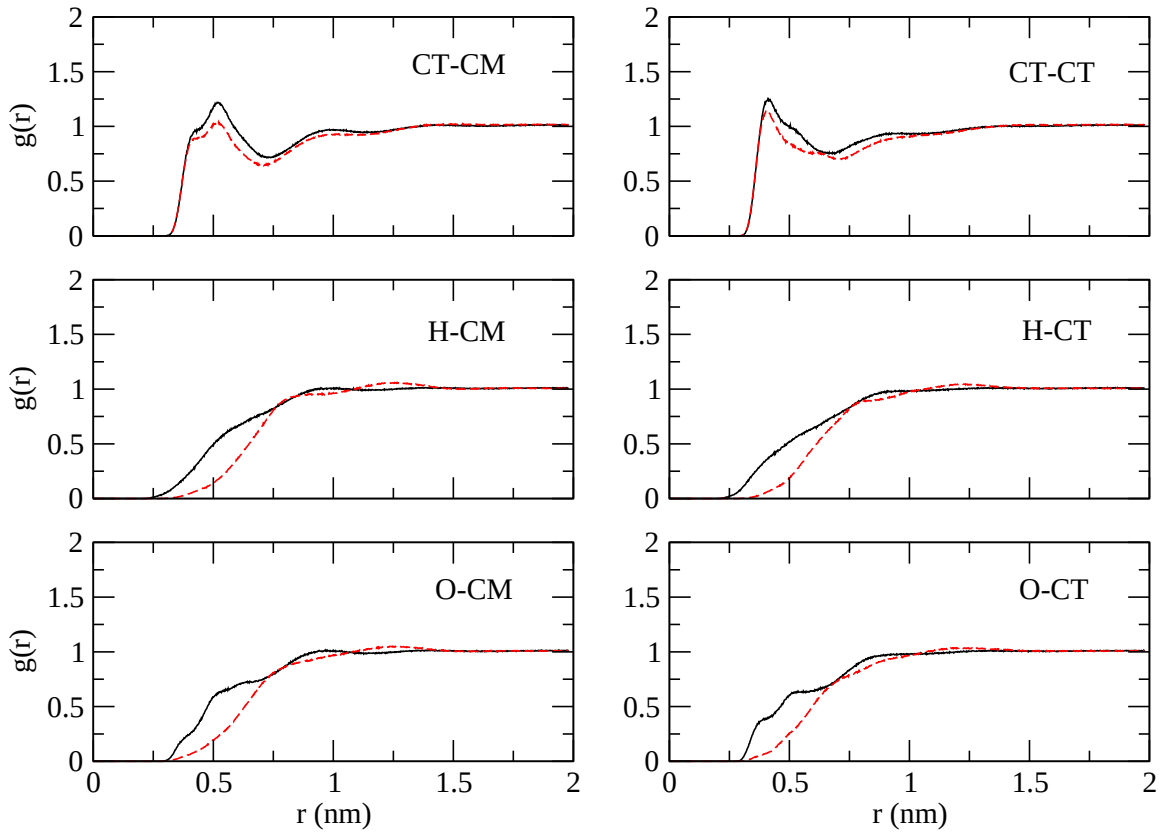

FIG. 30: Comparison of atomistic and CG site-site RDFs for the mixture of 130 butanol and 260 butane molecules not used in parameterizing the transferable CG potential functions. RDFs calculated from atomistic and CG MD simulations are presented as the solid black and dashed red curves, respectively. In each case, the first and second sites in each pair are from distinct butanol and butane molecules, respectively. CMA refers to the CM site next to the CT site in butanol, and CMB refers to the CM site next to the CP site in butanol.

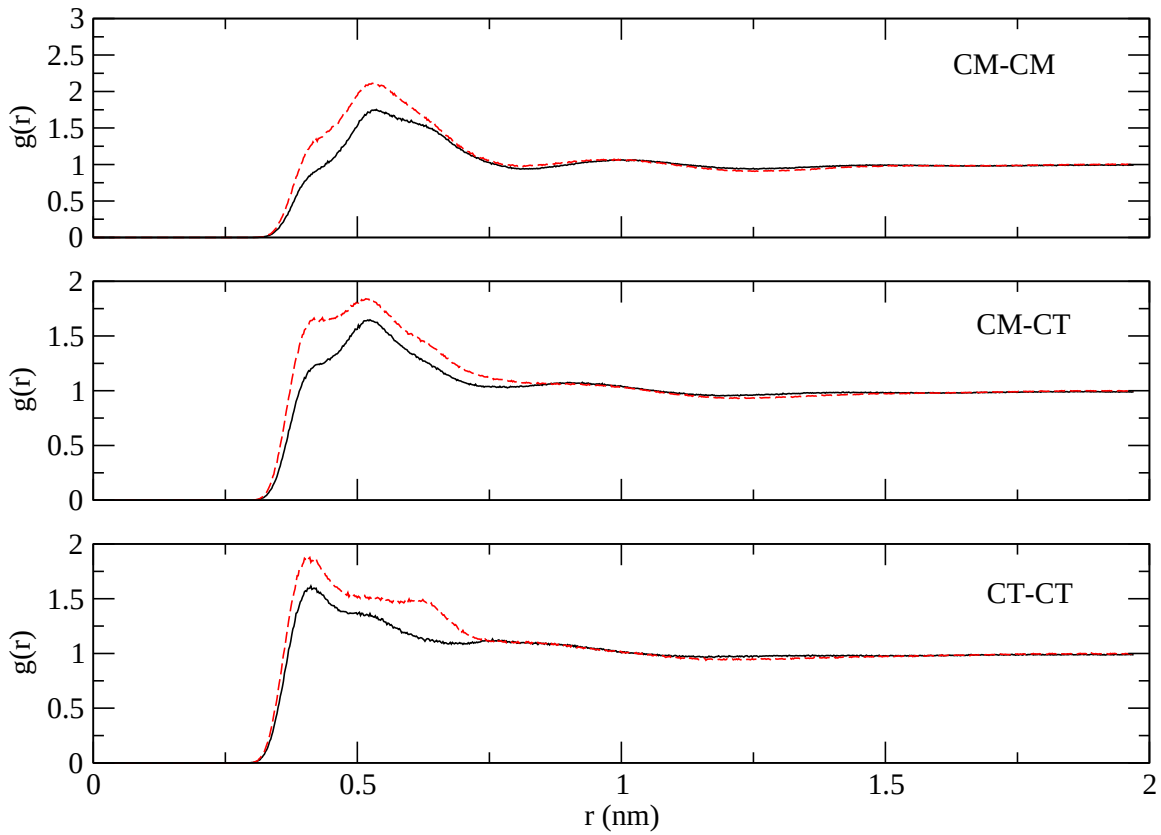

FIG. 31: Comparison of atomistic and CG site-site RDFs for the mixture of 266 butanol and 133 butane molecules not used in parameterizing the transferable CG potential functions. RDFs calculated from atomistic and CG MD simulations are presented as the solid black and dashed red curves, respectively. In each case, the sites in each pair are from distinct butane molecules.

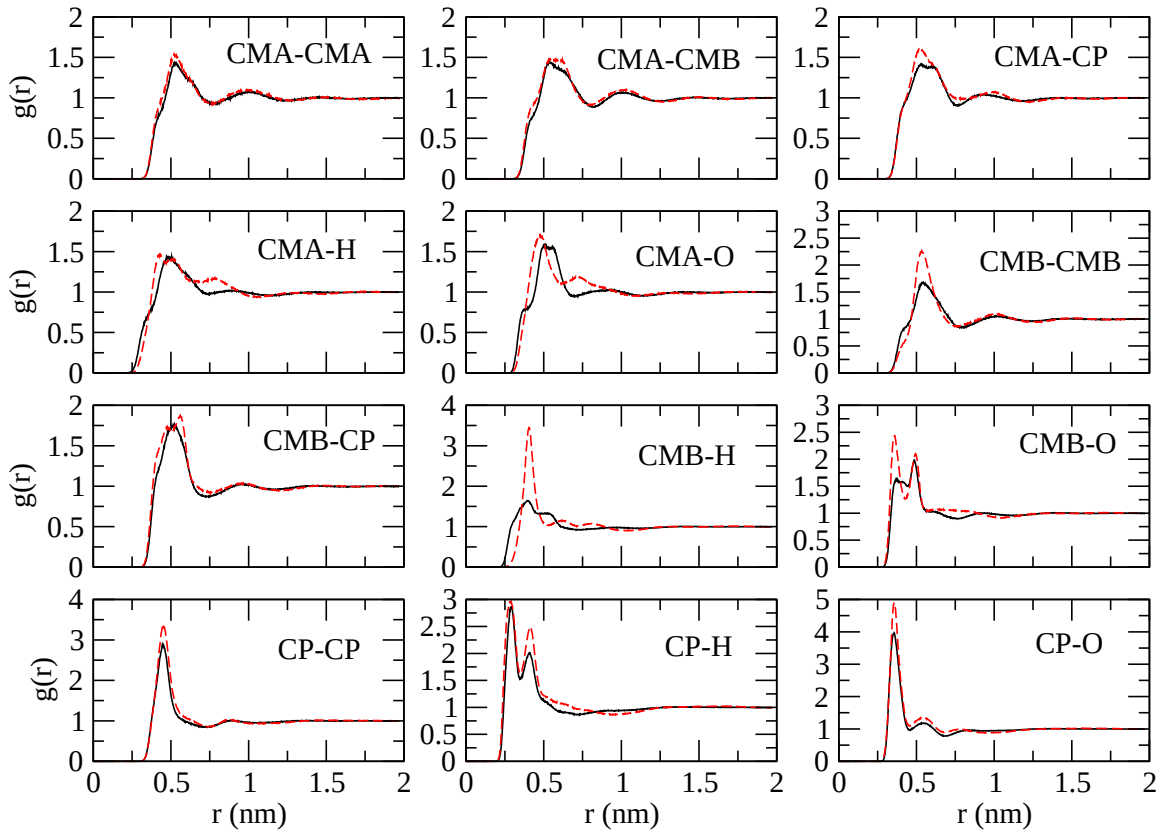

FIG. 32: Comparison of atomistic and CG site-site RDFs for the mixture of 266 butanol and 133 butane molecules not used in parameterizing the transferable CG potential functions. RDFs calculated from atomistic and CG MD simulations are presented as the solid black and dashed red curves, respectively. In each case, the sites in each pair are from distinct butanol molecules. CMA refers to the CM site next to the CT site in butanol, and CMB refers to the CM site next to the CP site in butanol.

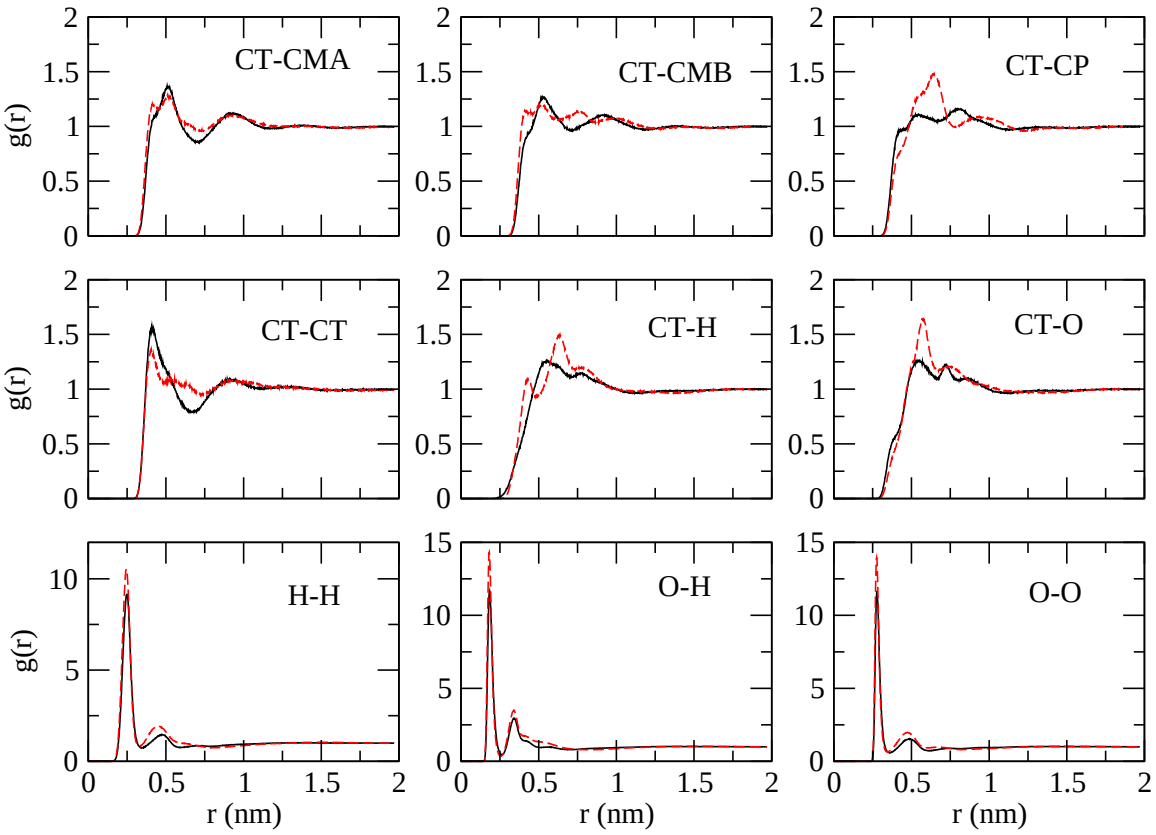

FIG. 33: Comparison of atomistic and CG site-site RDFs for the mixture of 266 butanol and 133 butane molecules not used in parameterizing the transferable CG potential functions. RDFs calculated from atomistic and CG MD simulations are presented as the solid black and dashed red curves, respectively. In each case, the sites in each pair are from distinct butanol molecules. CMA refers to the CM site next to the CT site in butanol, and CMB refers to the CM site next to the CP site in butanol.

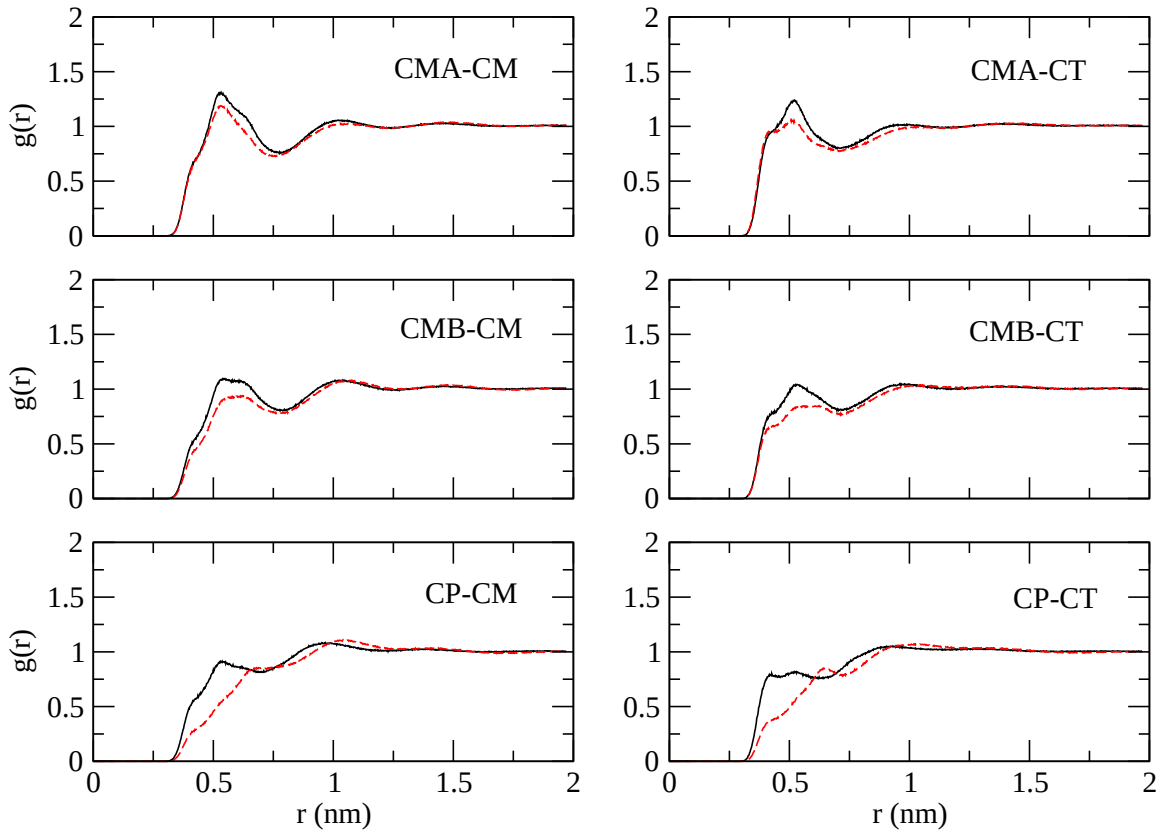

FIG. 34: Comparison of atomistic and CG site-site RDFs for the mixture of 266 butanol and 133 butane molecules not used in parameterizing the transferable CG potential functions. RDFs calculated from atomistic and CG MD simulations are presented as the solid black and dashed red curves, respectively. In each case, the first and second sites in each pair are from distinct butanol and butane molecules, respectively. CMA refers to the CM site next to the CT site in butanol, and CMB refers to the CM site next to the CP site in butanol.

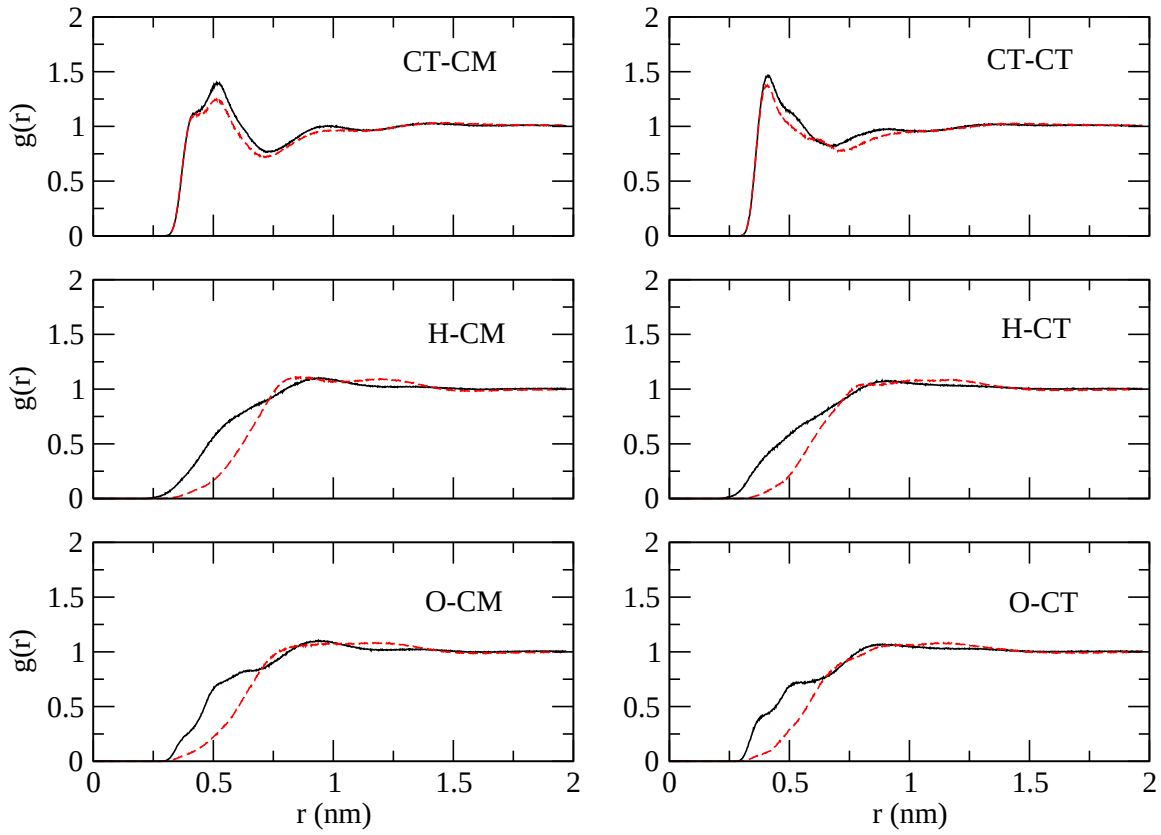

FIG. 35: Comparison of atomistic and CG site-site RDFs for the mixture of 266 butanol and 133 butane molecules not used in parameterizing the transferable CG potential functions. RDFs calculated from atomistic and CG MD simulations are presented as the solid black and dashed red curves, respectively. In each case, the first and second sites in each pair are from distinct butanol and butane molecules, respectively. CMA refers to the CM site next to the CT site in butanol, and CMB refers to the CM site next to the CP site in butanol.

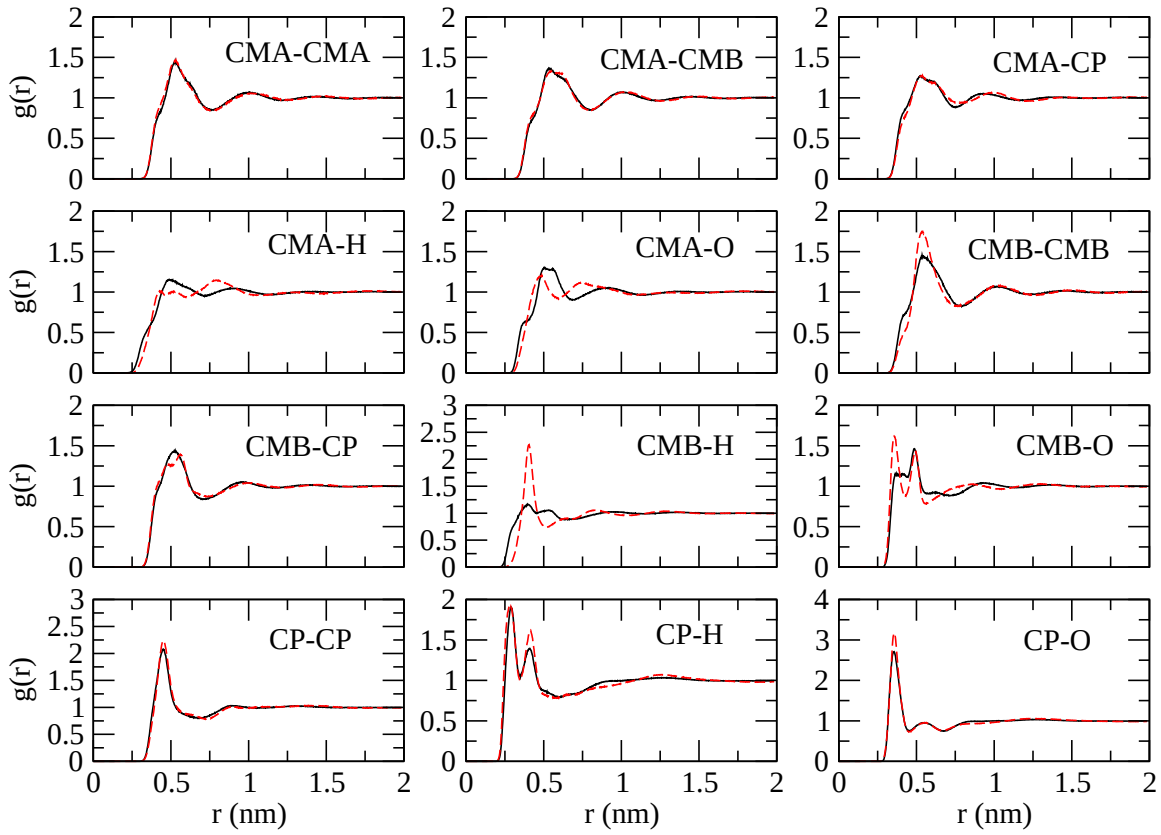

FIG. 36: Comparison of atomistic and CG site-site RDFs for the system of 420 butanol molecules not used in parameterizing the transferable CG potential functions. RDFs calculated from atomistic and CG MD simulations are presented as the solid black and dashed red curves, respectively. In each case, the sites in each pair are from distinct butanol molecules. CMA refers to the CM site next to the CT site in butanol, and CMB refers to the CM site next to the CP site in butanol.

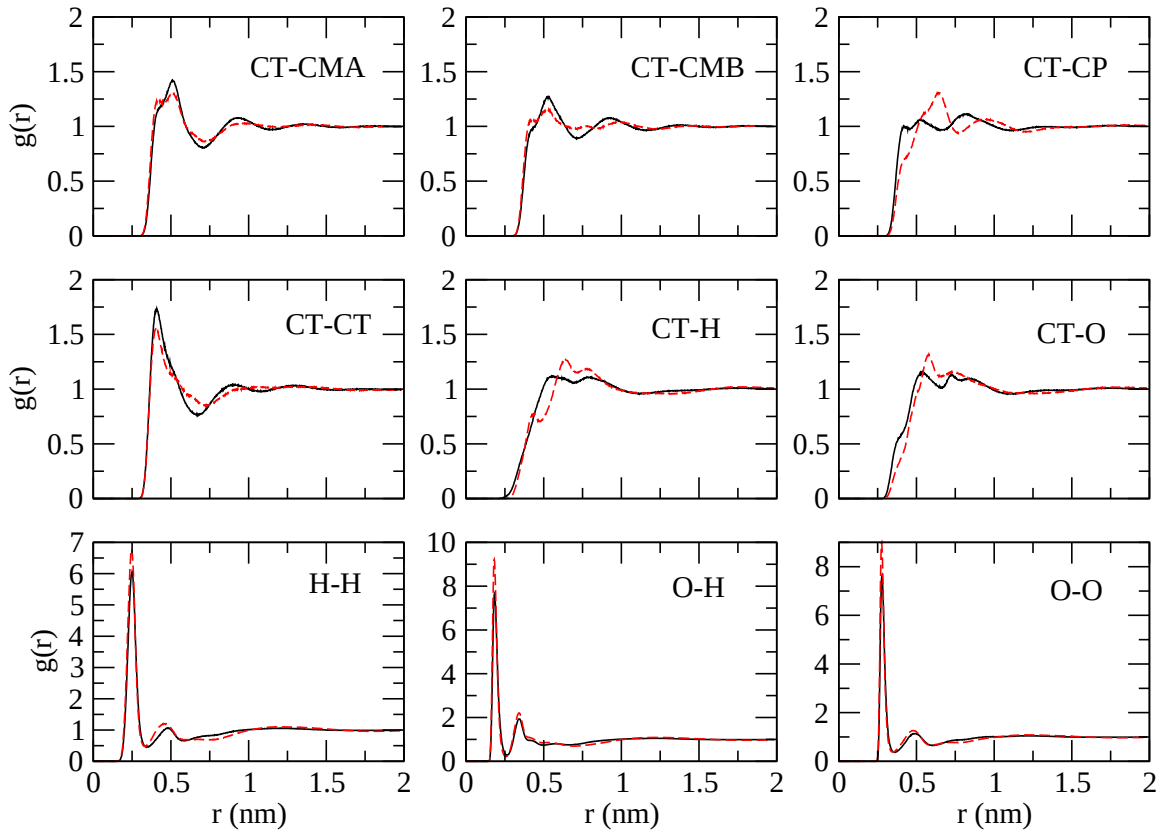

FIG. 37: Comparison of atomistic and CG site-site RDFs for the system of 420 butanol molecules not used in parameterizing the transferable CG potential functions. RDFs calculated from atomistic and CG MD simulations are presented as the solid black and dashed red curves, respectively. In each case, the sites in each pair are from distinct butanol molecules. CMA refers to the CM site next to the CT site in butanol, and CMB refers to the CM site next to the CP site in butanol.

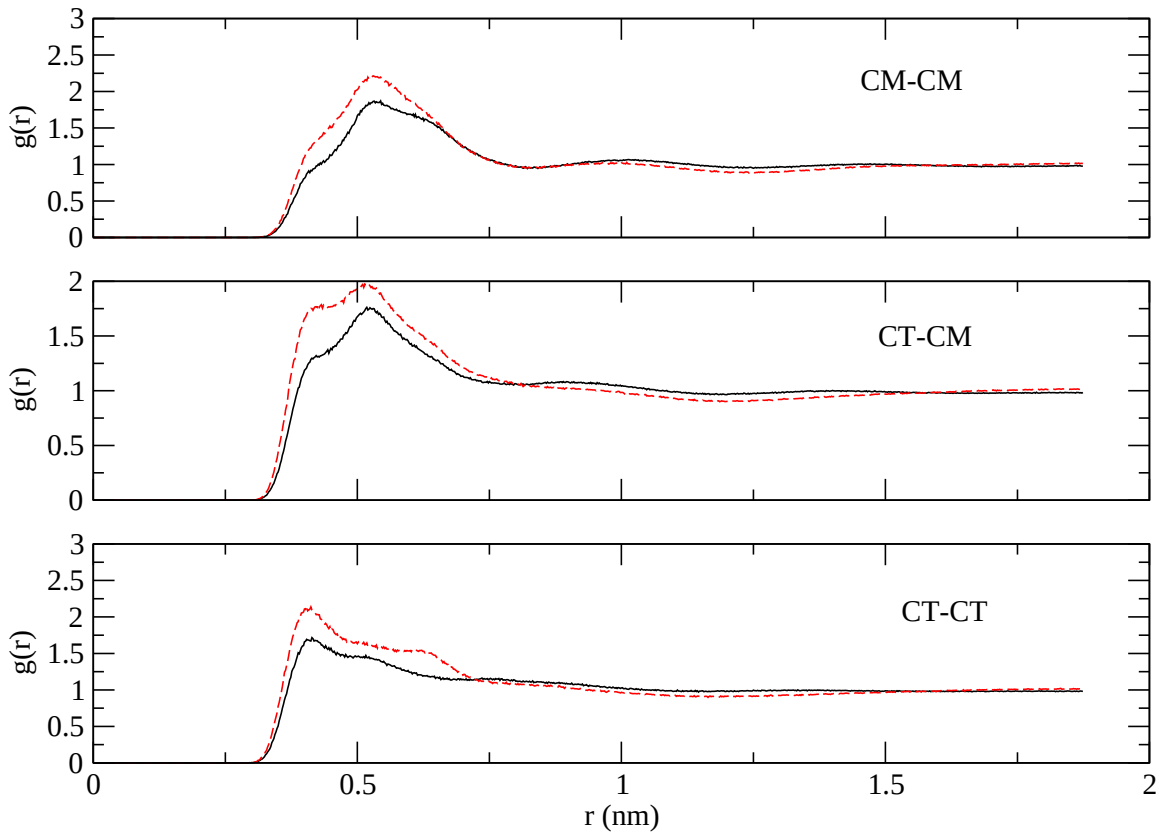

FIG. 38: Comparison of atomistic and CG site-site RDFs for the mixture of 300 propanol and 100 butane molecules not used in parameterizing the transferable CG potential functions. RDFs calculated from atomistic and CG MD simulations are presented as the solid black and dashed red curves, respectively. In each case, the sites in each pair are from distinct butane molecules.

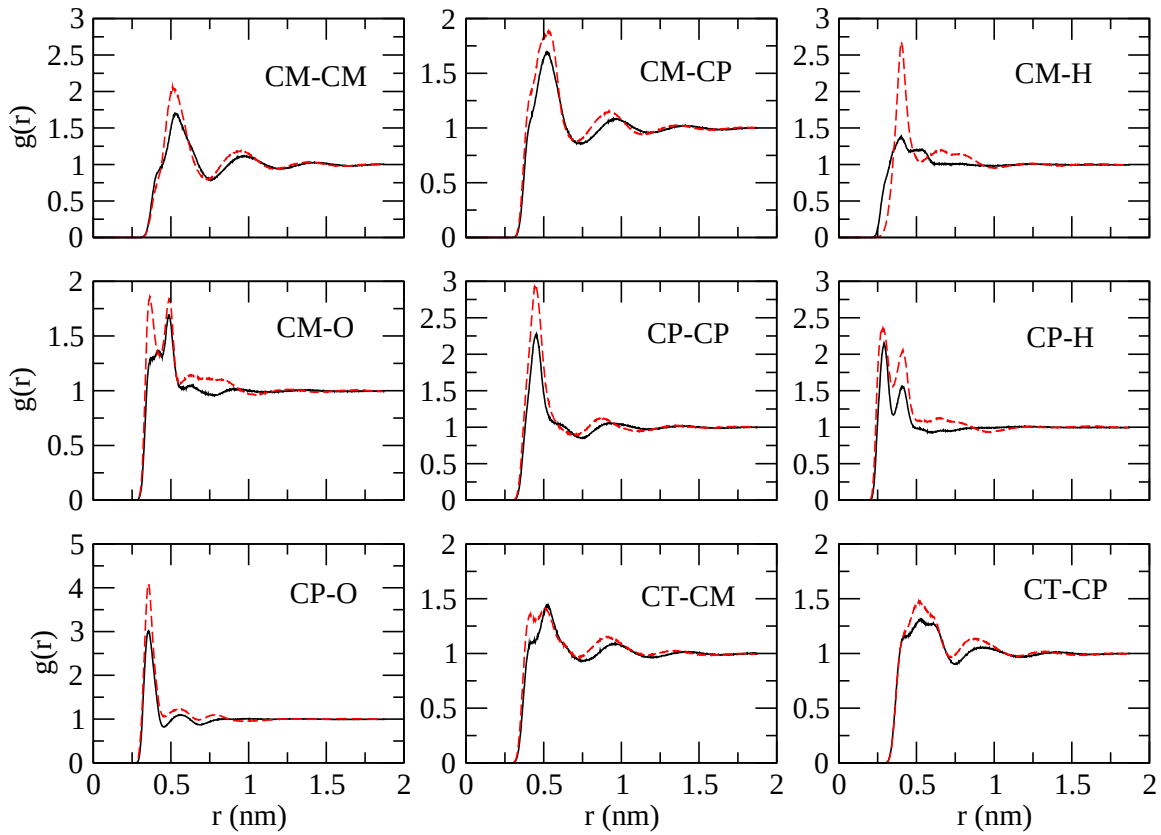

FIG. 39: Comparison of atomistic and CG site-site RDFs for the mixture of 300 propanol and 100 butane molecules not used in parameterizing the transferable CG potential functions. RDFs calculated from atomistic and CG MD simulations are presented as the solid black and dashed red curves, respectively. In each case, the sites in each pair are from distinct propanol molecules.

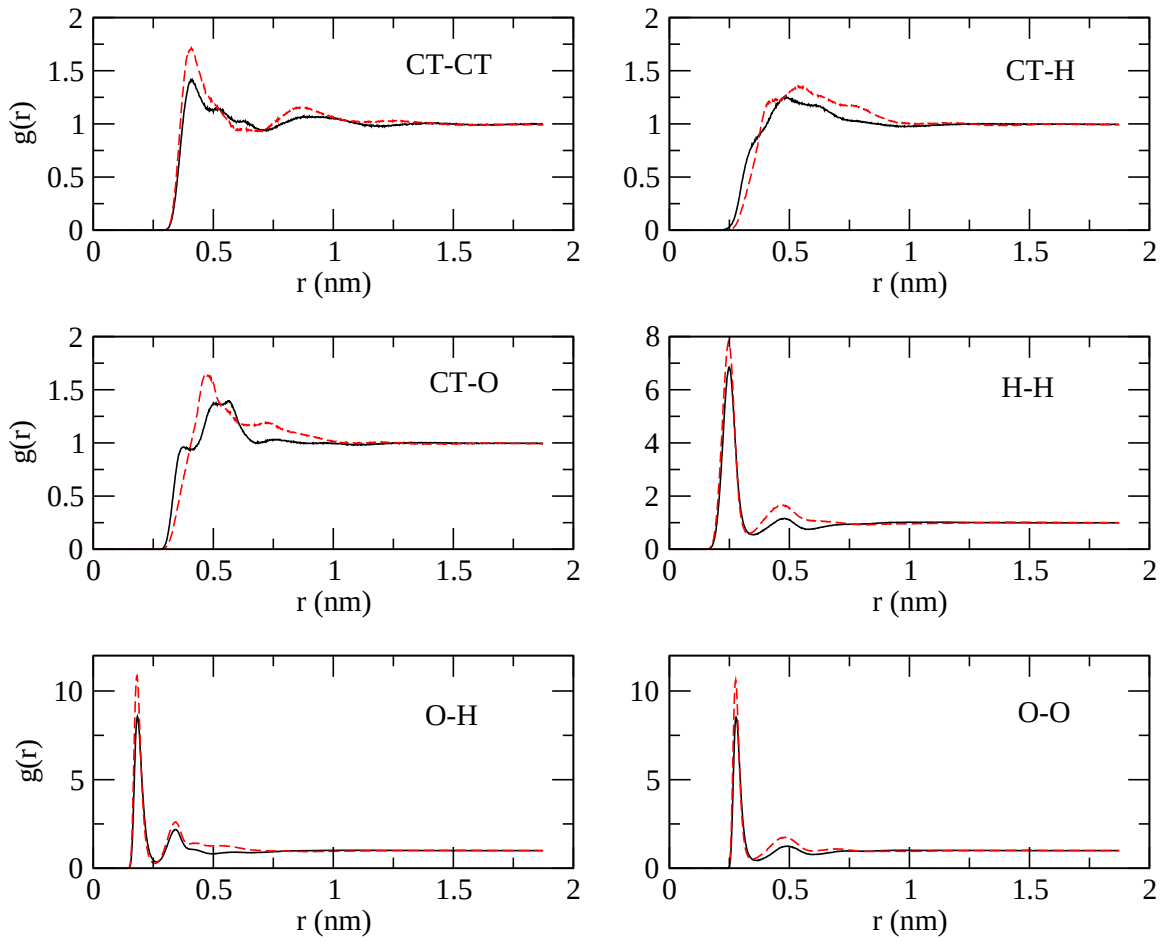

FIG. 40: Comparison of atomistic and CG site-site RDFs for the mixture of 300 propanol and 100 butane molecules not used in parameterizing the transferable CG potential functions. RDFs calculated from atomistic and CG MD simulations are presented as the solid black and dashed red curves, respectively. In each case, the sites in each pair are from distinct propanol molecules.

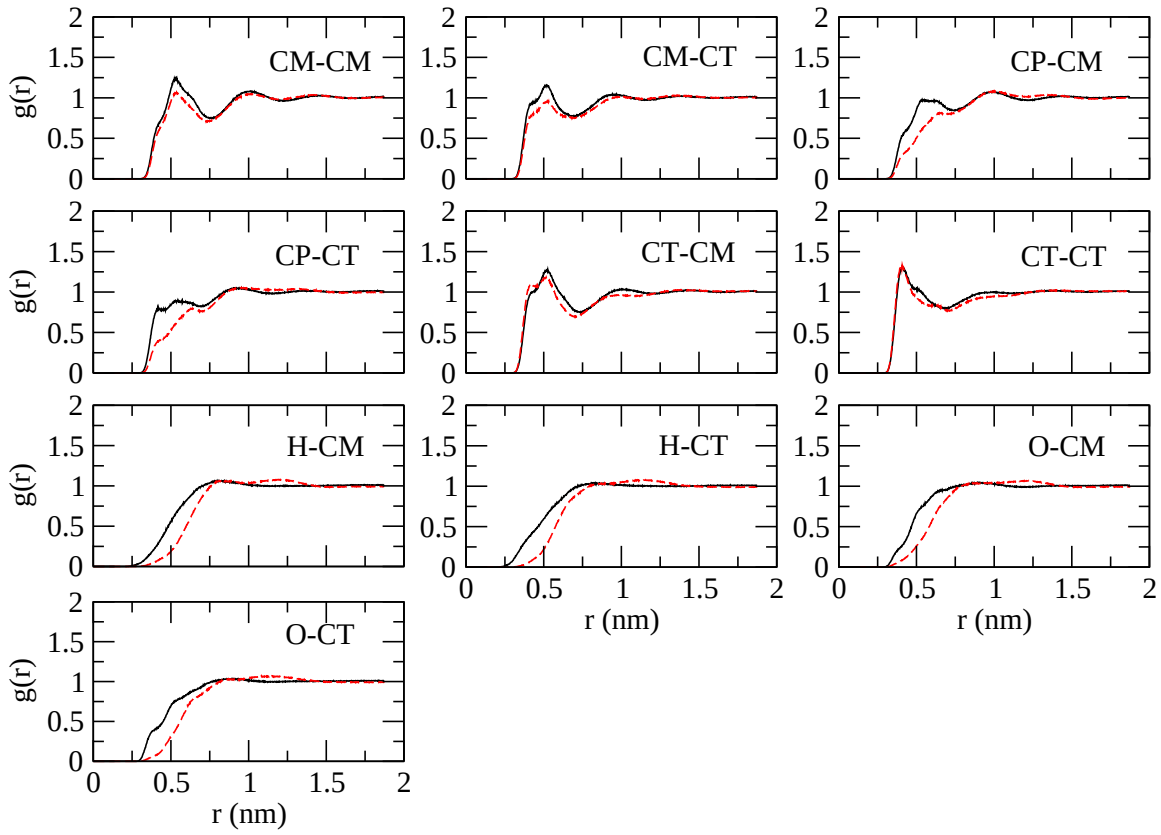

FIG. 41: Comparison of atomistic and CG site-site RDFs for the mixture of 300 propanol and 100 butane molecules not used in parameterizing the transferable CG potential functions. RDFs calculated from atomistic and CG MD simulations are presented as the solid black and dashed red curves, respectively. In each case, the first and second sites in each pair are from distinct propanol and butane molecules, respectively.

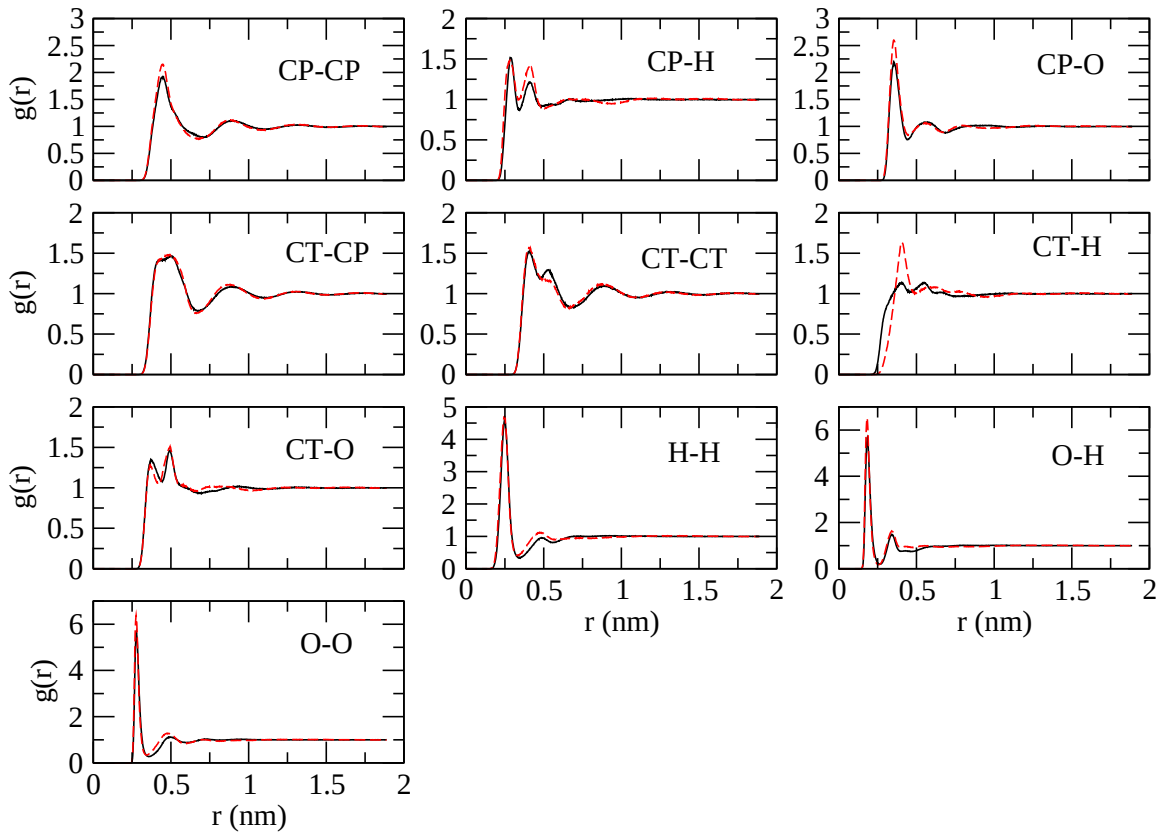

FIG. 42: Comparison of atomistic and CG site-site RDFs for the mixture of 375 ethanol and 125 butanol molecules not used in parameterizing the transferable CG potential functions. RDFs calculated from atomistic and CG MD simulations are presented as the solid black and dashed red curves, respectively. In each case, the sites in each pair are from distinct ethanol molecules.

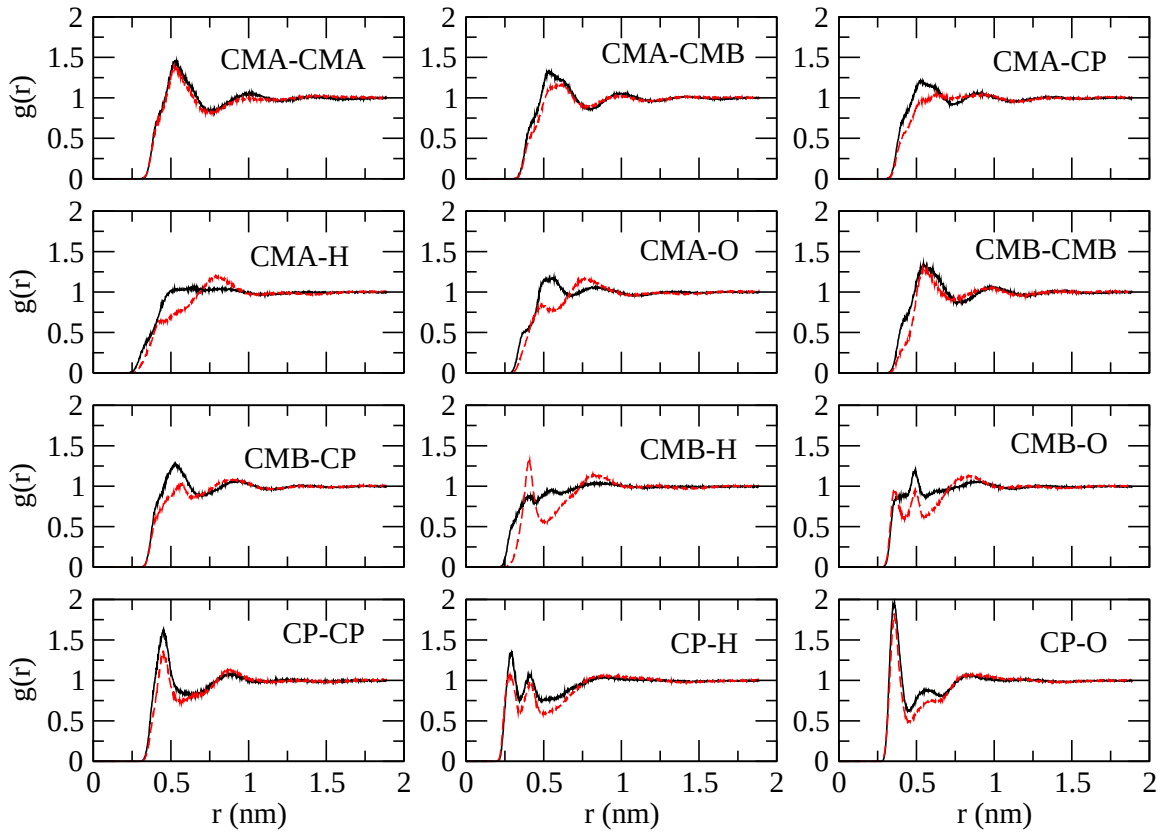

FIG. 43: Comparison of atomistic and CG site-site RDFs for the mixture of 375 ethanol and 125 butanol molecules not used in parameterizing the transferable CG potential functions. RDFs calculated from atomistic and CG MD simulations are presented as the solid black and dashed red curves, respectively. In each case, the sites in each pair are from distinct butanol molecules. CMA refers to the CM site next to the CT site in butanol, and CMB refers to the CM site next to the CP site in butanol.

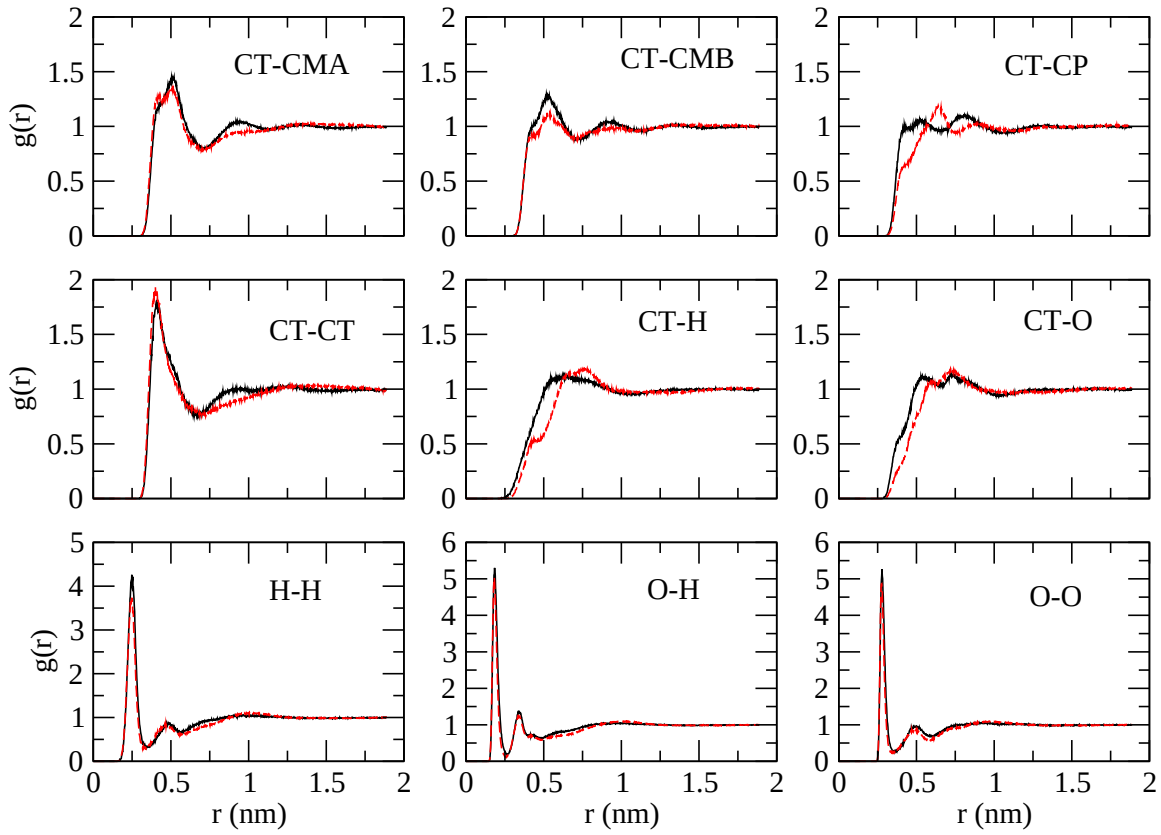

FIG. 44: Comparison of atomistic and CG site-site RDFs for the mixture of 375 ethanol and 125 butanol molecules not used in parameterizing the transferable CG potential functions. RDFs calculated from atomistic and CG MD simulations are presented as the solid black and dashed red curves, respectively. In each case, the sites in each pair are from distinct butanol molecules. CMA refers to the CM site next to the CT site in butanol, and CMB refers to the CM site next to the CP site in butanol.

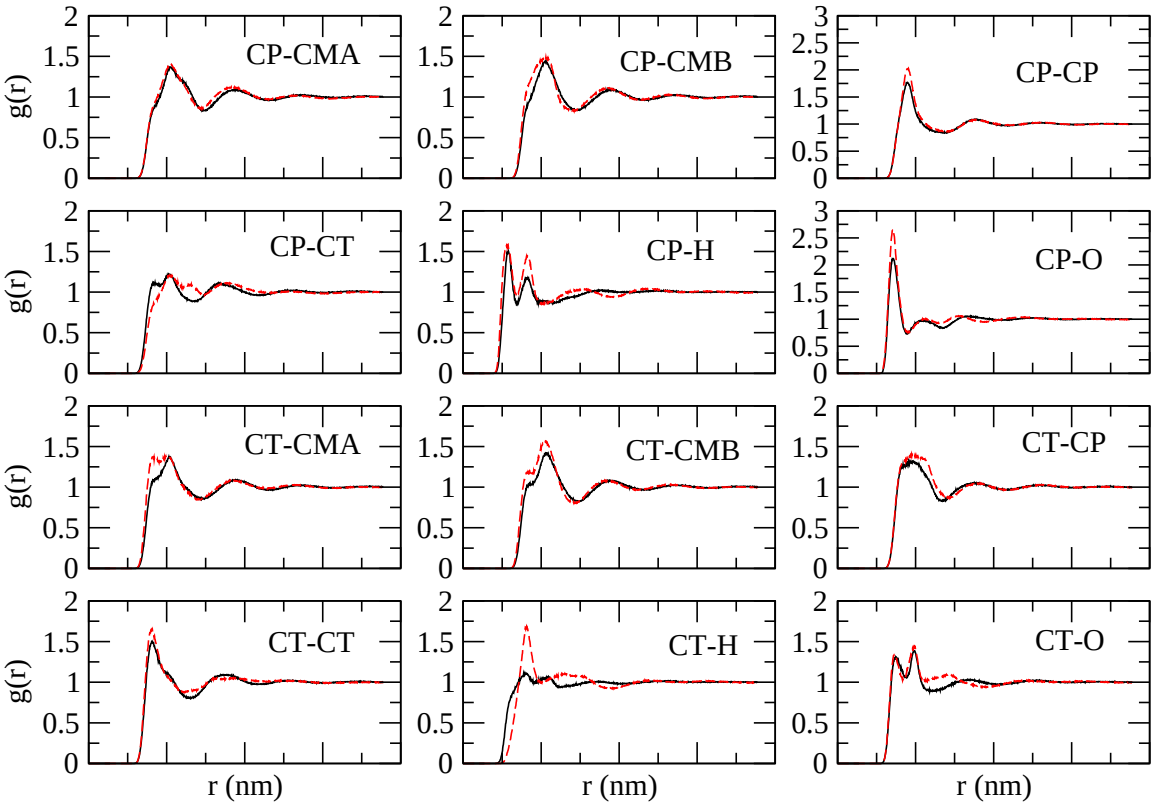

FIG. 45: Comparison of atomistic and CG site-site RDFs for the mixture of 375 ethanol and 125 butanol molecules not used in parameterizing the transferable CG potential functions. RDFs calculated from atomistic and CG MD simulations are presented as the solid black and dashed red curves, respectively. In each case, the first and second sites in each pair are from distinct ethanol and butanol molecules, respectively. CMA refers to the CM site next to the CT site in butanol, and CMB refers to the CM site next to the CP site in butanol.

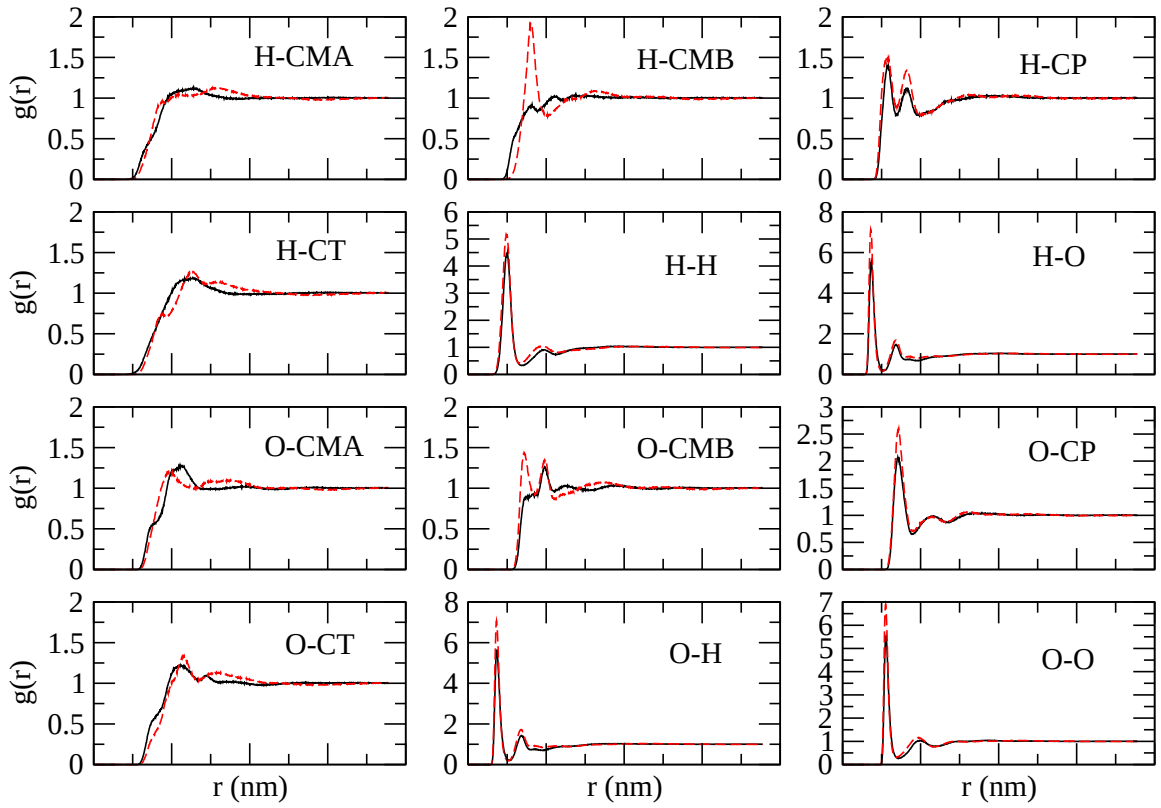

FIG. 46: Comparison of atomistic and CG site-site RDFs for the mixture of 375 ethanol and 125 butanol molecules not used in parameterizing the transferable CG potential functions. RDFs calculated from atomistic and CG MD simulations are presented as the solid black and dashed red curves, respectively. In each case, the first and second sites in each pair are from distinct ethanol and butanol molecules, respectively. CMA refers to the CM site next to the CT site in butanol, and CMB refers to the CM site next to the CP site in butanol.